A STUDY OF A LEAF MODEL USED IN THE SPRINKLING METHOD OF FREEZE PROTECTION OF PLANTS

Thesis for the Degree of Ph. D.
MICHIGAN STATE UNIVERSITY
Jerry Lee Chesness
1965

THESIS
C.3
3 1293 30029 7110

ABSTRACT

A STUDY OF A LEAF MODEL USED IN THE SPRINKLING METHOD OF FREEZE PROTECTION OF PLANTS

by Jerry Lee Chesness

The need for an effective method of preventing agricultural crops from freezing has led to extensive research into the sprinkling method of freeze protection. Some of this research has been directed toward the derivation of a sprinkling rate prediction equation based on heat transfer theory applied to models of various plant structural parts.

In this investigation a theoretical and experimental analysis was made of the commonly accepted leaf model, a thin flat plate, under simulated field conditions. Convective and mass-transfer heat losses from a flat plate were measured in a wind tunnel with controlled air temperatures between 15 and 32 F, air velocities between 50 and 900 ft/min, and relative humidity between 35 and 75 percent. Radiation losses were not considered in this study. Free stream turbulence in the wind tunnel was held to a maximum of 4.0 percent.

Jerry Lee Chesness

Phase One of the study was concerned with determining the convective heat loss equation for a thin uniformly heated flat plate with laminar air flow parallel to its surface. The plate was constructed from two 6 in. x 6 in. x .051 in. pieces of aluminum with thermocouples imbedded in the surface and a heating element sandwiched between them. It was found that the heat loss can be predicted from an equation differing only slightly from the theoretical equation for a plate with a continuously varying surface temperature.

In Phase Two the rate of heat loss due to the mass transfer of water vapor from a stationary water surface into a laminar air stream was determined. Measurements were made of the actual quantity of water removed per unit time from the cloth covered surface of an 8 in. x 8 in. x 3/4 in. heated (to prevent the water surface from freezing) insulated plastic tray.

Phase Three involved the continuous sprinkling of a 4 in. x 4 in. x 1/8 in. leaf model with laminar air flow occurring over both surfaces (angle of incidence = 0). The leaf model was fitted with thermocouples to provide a measure of the local surface temperature on the underside, the mean water film temperature on the upper surface, and the mean temperature of the water leaving the surface. The sprinkling rate and mean water drop temperature (at the leaf model surface) was measured by an insulated catchment tray. The equation for the average film heat transfer coefficient

Jerry Lee Chesness

was derived for the condition of a flowing water film on the leaf model surface. Using this coefficient in the convective and mass-transfer heat loss equations for the upper plate surface, combined with the convective heat loss equation from Phase One for the underside and the heat gained from the sensible heat of the sprinkled water resulted in a theoretical value for the water application rate which correlated with the measured value. The theoretical water application rate can therefore be predicted if the air velocity, air temperature, relative humidity, local surface (un-wetted) temperature, and mean water film temperature are known.

Approved Ernest N. Bodine
Major Professor

Approved Carl W. Hall
Department Chairman

Date Jan 10, 1966

A STUDY OF A LEAF MODEL USED IN THE SPRINKLING METHOD OF FREEZE PROTECTION OF PLANTS

By

Jerry Lee Chesness

A THESIS

Submitted to
Michigan State University
in partial fulfillment of the requirements
for the degree of

DOCTOR OF PHILOSOPHY

Department of Agricultural Engineering

1965

ACKNOWLEDGMENTS

This study was carried out under the guidance and supervision of E. H. Kidder (Agricultural Engineering) whose interest and encouragement has been most gratifying.

I am deeply indebted to Dr. A. M. Dhanak (Mechanical Engineering) for his brilliant council and guidance in the application of heat transfer theory to this study.

To Dr. C. E. Cutts (Civil Engineering), and Dr. F. H. Buelow (Agricultural Engineering) the author expresses his gratitude for their time, professional interests, and constructive criticisms.

This dissertation is dedicated to my wife, Betty, whose unfailing support and endless faith enabled me to attain this goal.

TABLE OF CONTENTS

	Page
LIST OF FIGURES	v
LIST OF TABLES	viii
NOMENCLATURE	x
I. INTRODUCTION	1
1.1 Objectives	2
II. REVIEW OF LITERATURE	3
III. ANALYSIS	8
3.1 General Background	8
3.2 Convection	12
3.3 Mass-Transfer	21
3.4 Sprinkling the Leaf Model	23
IV. EXPERIMENTAL EQUIPMENT	27
4.1 Wind Tunnel	27
4.1.1 Temperature	29
4.1.2 Velocity	31
4.1.3 Turbulence	33
4.1.4 Relative Humidity	33
4.2 Heated Flat Plate	35
4.3 Mass-Transfer	40
4.4 Leaf Model	44
V. EXPERIMENTAL PROCEDURE	50
5.1 Convection	50
5.2 Mass-Transfer	51
5.3 Sprinkling the Leaf Model	54

Page

VI. DISCUSSION OF RESULTS 57

6.1 Convection 57
6.2 Mass-Transfer 61
6.3 Sprinkling the Leaf Model 65

VII. CONCLUSIONS 81

SUGGESTIONS FOR FUTURE STUDIES 84

APPENDICES 85

REFERENCES 115

LIST OF FIGURES

Figure		Page
1	Flow boundary layer and thermal boundary layer on a flat plate heated over its entire surface	14
2	Approximation of continuously varying wall temperature by straight line segments . .	21
3	Wind tunnel layout	28
4	Inlet section of wind tunnel	30
5	Temperature recording potentiometers . . .	30
6	Hot-wire anemometer, root-mean-square voltmeter, and oscilloscope	34
7	Relative humidity indicator and sensors . . .	34
8	Dimensional view of heated flat plate	36
9	Cutaway view of heated flat plate	38
10	Heated flat plate located in test area	39
11	Equipment set-up for measuring mass-transfer	39
12	Dimensional view of mass-transfer tray . .	41
13	Cutaway view of mass-transfer tray	42
14	Leaf model in test area of wind tunnel . . .	45
15	Tray for measuring water application rate and drop temperature	45

Figure		Page
16	Wind tunnel with sprinkling equipment attached	47
17	Sprinkling tower and water control assembly	47
18	Comparison of measured and calculated average film heat-transfer coefficients in laminar flow over a flat plate	60
19	Dimensionless mass-transfer coefficient for a flat surface evaporating water into a laminar air flow	64
20	A comparison of the experimental and theoretical water application rates	67
21	Average film heat-transfer coefficients in laminar flow over a flat plate	76
22	A comparison of the experimental and theoretical water application rates with the theoretical water application rate calculated for a flat plate surface covered by a moving water film	77
23	Dimensionless mass-transfer coefficient for a flat surface evaporating water into a laminar air flow	78
24	Dimensionless water application rate number for the leaf model in laminar air flow parallel to its surface	79
25	Empirical correlation curve for determining $\Delta T_p'$ when the air, water film, and local plate temperatures are known	80
26	Flow boundary layer over a water film on a flat plate	85
27	Water film on a flat plate	91

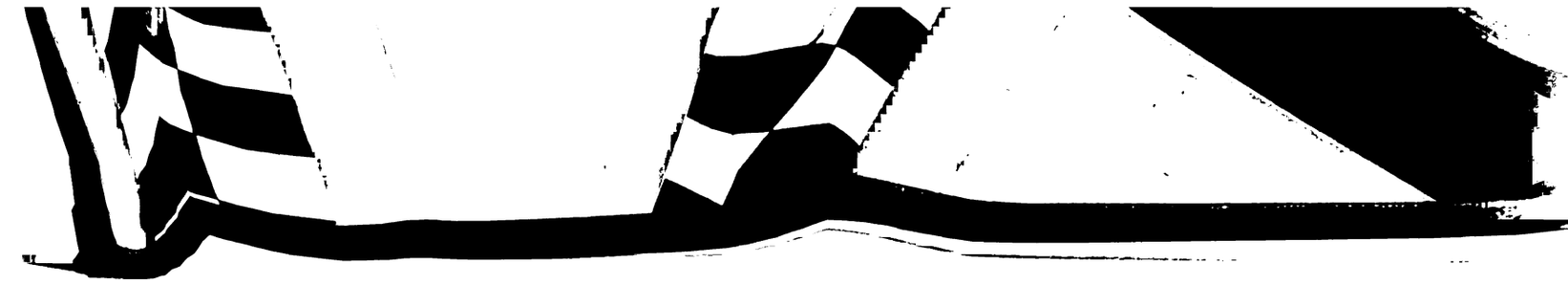

Figure		Page
28	Approximation of continuously varying plate surface temperature by straight line segments for convection test number 8 . .	95
29	Calibration curve for determining the quantity of water removed from the mass-transfer tray during a test	100
30	Approximation of continuously varying plate surface temperature by straight line segments for sprinkling test 22	104
31	The effect of air velocity on the quantity of water collected over a five minute period for sprinkling rate determinations (tests 21 through 26)	107

LIST OF TABLES

Table		Page
1	Summary of convection tests	59
2	Summary of mass-transfer tests	63
3	Summary of sprinkling tests	66
4	Sprinkling data analyzed on the basis of the theoretical relationships developed for a flowing water film on a flat plate	73

LIST OF APPENDICES

Appendix		Page
A.	Theoretical derivation of the average film heat-transfer coefficient over a flowing water film	85
B.	Sample calculations	93
C.	Propagation of errors for the theoretical water application rate equation	110

NOMENCLATURE

C_p	specific heat, Btu/lb_m F
D	diffusion coefficient, ft^2/min
d	diameter of drops, in.
f	sprinkling frequency, min
$\bar{h}_c$	average convective heat transfer coefficient for a flat plate with a constant surface temperature, Btu/min ft^2 F
$\bar{h}_c'$	average convective heat transfer coefficient for a flat plate with a continuously varying surface temperature, Btu/min ft^2 F
$\bar{h}_m$	average mass-transfer coefficient, ft / min
H_v	latent heat of vaporization, Btu/lb
i	ice load, lb
I	current to heating wire, milliamperes
k	thermal conductivity, Btu/min ft F
L	length of leaf, ft
m_s	rate of mass transfer, lb_m/min

P_a	vapor pressure of the air, lb/ft^2
P_s	vapor pressure at the water surface, lb/ft^2
q_{ct}	total heat removed by convection, $Btu/min\ ft^2$
q_c	heat removed by convection from a flat plate with a constant surface temperature, $Btu/min\ ft^2$
q_c'	heat removed by convection from a flat plate with a continuously varying surface temperature, $Btu/min\ ft^2$
q_m	heat removed by mass-transfer, $Btu/min\ ft^2$
q_w	heat added through sprinkling, $Btu/min\ ft^2$
Q_e	measured heat loss from the flat plate, defined by equation (5.1.4), Btu/lb
R	universal gas constant, $ft/^oR$
r	radiation characteristics
RH	relative humidity, percent
SE_y	standard error of estimate for the y ordinate values
T	absolute temperature of the water film, R
t_a	local air temperature, F
t_p	local un-wetted plate surface temperature, F
T_a	free stream air temperature, F
T_d	mean temperature of the drops striking the surface of the water film on the leaf model, F

T_m = $(T_s - T_a)/2$, mean temperature for evaluating the fluid properties over the water film, F

T_m' = (average plate surface temperature - T_a) /2, mean temperature for evaluating the fluid properties over the plate surface, F

$\Delta T_p'$ plate surface temperature defined by equation (6.1.1), F

t_s local water film temperature, F

T_s mean water film temperature, F

T_w mean temperature of the water leaving the leaf model surface, F

ΔT_w = $T_d - T_w$

u velocity at any point in the hydrodynamic boundary layer, ft/min

U_a free stream velocity of the air, ft/min

V voltage to heating wire, volts

w_e measured water application rate, in./min

w_t theoretical water application rate, in./min

W dimensionless water application rate number defined by equation (3.4.4)

x, y, z rectangular coordinates

δ hydrodynamic boundary layer thickness, ft

δ_t thermal boundary layer thickness, ft

ζ ratio of δ_t/δ

ν kinematic viscosity, ft^2/min

η ratio of y/δ_t

μ absolute viscosity, $lb_m/ft^2 min$

ρ mass density, lb_m/ft^3

$\alpha = \frac{k}{\rho\ Cp}$, thermal diffusivity, ft^2/min

$\overline{Nu} = \frac{\bar{h}_c L}{k}$, Nusselt number

$\overline{Nm} = \frac{\bar{h}_m L}{k}$, dimensionless mass-transfer number

$Re_L = \frac{U_a L}{\nu}$, Reynolds number

$Pr = \frac{Cp\ \mu_a}{k}$, Prandtl number

$Sc = \frac{\nu}{D}$, Schmidt number

$Le = \frac{\alpha}{D}$, Lewis number

I. INTRODUCTION

Every year partial and in some cases total destruction of agricultural crops by freezing exacts a heavy economic toll from the farmers in this country and abroad. As the crop yields per acre increase along with their increased value the necessity of insuring these yields against loss by freezing increases. A number of methods for preventing freeze damage to agricultural crops have been tried, each meeting with varied degrees of success.

The sprinkling of water on agricultural crops as a method of preventing freeze damage has been successfully applied for over 30 years. The success of this method has been somewhat limited with respect to the types of crops it can protect, and the nature and severity of the freeze conditions encountered. The research work leading to the adoption and utilization of the sprinkling method has been primarily of the field experimentation type, directed toward obtaining a broad working knowledge of the method. Precise theoretical descriptions of the sprinkling process in the field have not been obtained owing to the almost inseparable manner in which the effects of plant and environment on the heat and mass transfer process are interwoven. If the limits and accurate application of the sprinkling

method are to be obtained a concise description of the physical processes leading to a quantitive sprinkling rate prediction equation must be developed. This approach has, in recent years, been undertaken by researchers who have applied heat transfer theory to geometric models representing various plant structural parts. The prediction equations arrived at through these analyses have met with a limited degree of success when applied to the actual sprinkling of plants in the laboratory and field. The limited degree of success may be attributed to the fact that the prediction equations have not been experimentally verified for the models postulated. It is in this area of the sprinkling method of freeze protection research that this study will be conducted.

1.1 Objectives

The overall objective of this study is to examine theoretically and experimentally a leaf model under freeze conditions representing the actual field conditions encountered by the plant. This overall objective can be divided into three separate objectives or phases of study:

1. The convective heat losses from a heated flat plate under freezing conditions will be measured.
2. The mass-transfer from a stationary free water surface subjected to freezing conditions will be measured.
3. The sprinkling rate for a leaf model subjected to freezing conditions will be measured.

II. REVIEW OF LITERATURE

The first systematic investigations of the sprinkling method of freeze protection for agricultural crops was carried out in 1938 by Kessler and Kaempfert (1949). Investigations were conducted by Kidder and Davis (1956) and Braud and Hawthorne (1965) on the sprinkling rate and frequency required to protect strawberries. Sprinkling rates for the protection of blueberries were determined by Shultz and Parks (1957) in California. Rogers (1952) investigated the physical tolerance of plant tissues to freezing temperatures. Rogers et al. (1954) conducted research in England on the application of the sprinkling method of freeze protection to deciduous fruit buds. Von Pogrell and Kidder (1959) investigated the effect of drop size and distribution, air temperatures, application rates, and spraying frequencies on the frost protection of plant leaves. Gerber and Harrison (1963) reported on the results of employing the sprinkling method of freeze protection on Citrus in Florida. Wheaton (1959) determined experimentally the effect of application rate and spraying frequency on the freeze protection of bean leaves.

The research work carried out by these and other investigators has led to an overall understanding of the variables involved in the sprinkling method of freeze protection and their inter-

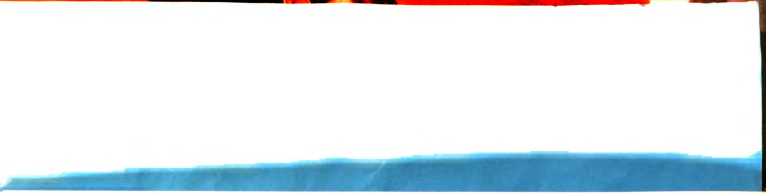

relationships. Strawberries and other low growing crops can be protected from temperatures as low as 20 F (produced by radiation freezes) with sprinkling rates in the neighborhood of 0.1 in./hr. As the quantity of heat removed from the plant surface by radiation, convection, and evaporation increases the sprinkling rate and spraying frequency must be increased in order to prevent freeze damage. Some approximate limits have been established for this method of freeze protection based on the adverse effects of soil saturation accompanying prolonged sprinkling, inability to supply sufficient heat for severe wind borne freezes, and damage to the structural portions of the plant produced by heavy ice loads.

A few researchers have attempted a purely theoretical approach to procuring a sprinkling rate prediction equation which takes into account the many variables involved. Geometrical models have been proposed to represent various structural parts of a plant. The three basic models are: (1) a flat plate to represent a leaf; (2) a sphere to represent a bud or individual fruit; and (3) a cylinder to represent a shoot or branch. Applying heat transfer theory to these models has resulted in the postulation of theoretical prediction equations for the sprinkling rate.

Nieman (1958) described the various phases of heat transfer, radiation, convection, and evaporation and how they affect the heat balance of the plant.

Beahm (1959) calculated the theoretical water application rates required to protect various size flat plates, cylinders, and spheres for various convective, evaporative, and radiative heat losses. The author did not attempt to verify these values for the model or the portion of the plant represented by the model. Beahm arrives at the following prediction equation for a flat plate with an angle of incidence equal to zero, laminar air flow, constant surface temperature, constant radiative heat loss, constant plate length, evaporation from top surface only, 100 percent of sprinkled water freezing on plate surface, and 100 percent relative humidity;

$$w = \frac{28 + h[2931.5 - T_a + 102(P_s - P_a)]}{780}$$

In this equation,

w = water application rate, in./hr

h = film coefficient from leaf to air, Btu/hr ft^2 F

T_a = free stream air temperature

P_s = saturated vapor pressure at the plate surface, lb/ft^2

P_a = vapor pressure at the plate surface, lb/ft^2

Businger (1963) made a theoretical study of the heat transfer process taking place on a flat plate and a sphere. Applying the energy balance on the flat plate results in the following sprinkling rate prediction equation

$$w = \alpha \frac{2}{L_i} (h_r + h + h_e) (T_m - T_l)$$

where

w = the water application rate

α = ratio of the actual quantity of water required to the theoretical quantity required ($\alpha > 1$)

L_i = latent heat of fusion of water

h_r = coefficient of radiative heat transfer

h = coefficient of convective heat transfer

h_e = coefficient of evaporative heat transfer

T_m = minimum tolerable leaf temperature

T_l = leaf temperature

The author assumes that both the upper and lower leaf surfaces are covered with a continuous water film and that both surfaces have a constant temperature. Comparing experimental values with theoretical values calculated from the above equation results in a value of 1.5 for α. This type of correlation offers no confirmation as to the validity of the theoretical prediction equation since any unaccounted or inaccurately accounted for heat losses will remain hidden in the value of α.

Gates and Benedict (1963) observed the free convection from leaves in still air my means of schlieren photographs of broad-leaved trees. A quantitative measure of the rate at which heat was convected away from the leaf was obtained by photographing the size

of the convection plume, measuring its rate of flow by means of movie photography, and measuring the temperature of the plume with a fine thermocouple. Their observations of free convection from broad-leaved plants confirmed the values predicted using heat transfer theory for heated plates.

III. ANALYSIS

3.1 General Background

A plant located in its natural environment gains or loses heat from or to its surroundings by three separate physical processes: (1) conduction and convection; (2) evaporation and transpiration; and (3) radiation exchange.

Conduction is a process by which heat flows from a region of higher temperature to a region of lower temperature within a medium or between different mediums in direct physical contact. For plants this medium can be the solid material forming its physical structure, the water films forming on its surface, and the air surrounding it.

Radiation is a process by which heat flows from a high temperature body to a lower temperature body when they are separated in space. Although the term "radiation" is generally applied to all kinds of electromagnetic-wave phenomena, our concern in heat transfer is only with those phenomena which are the result of temperature. This energy is called "radiant heat."

Convection is a process of energy transport by the combined action of heat conduction, energy storage, and mixing motion. Convection is the mechanism of energy transfer between the solid surfaces of the plant and the surrounding air mantle.

Under freezing conditions the plant loses heat to its surroundings by these heat transfer processes singularly or in combination. The physiological make up of each plant species dictates what minimum temperature each segment of the plant structure can withstand before destruction of the cells occurs. In general, however, investigations by Beahm (1959), Wheaton (1959), Rogers (1952), and others indicate that the minimum temperature is below 32 F (around 31 F).

In the sprinkling method of frost control the heat lost from the plant to its surroundings is replaced by the heat in the water. This heat is in the form of sensible heat and the heat of solidification (freezing). Since the minimum temperature which the plant can tolerate is approximately 31 F, no freeze damage occurs when ice forms on the plant surface if the ice coat is maintained at a temperature above 31 F.

It should be pointed out that when the plant surface is covered with a water film from sprinkling and exposed to a moving air mass an additional heat loss phenomenon occurs. Under these conditions the mass-transfer (evaporation) of water vapor from the water surface into the moving air stream takes place with a subsequent heat loss termed "latent heat of vaporization."

The effects of plant and environment on the heat transfer in which both are involved are interwoven to such an extent that they should be described together. However, in order to determine the

basic heat transfer processes involved and give a description of these processes, it is necessary to separate in as much as possible these interwoven effects. To ultimately meet this objective it is necessary to divide the structural parts of the plant into shapes which are geometrically similar and for which a model can be postulated.

This investigation will be concerned only with that structural portion of the plant called the leaves. Consider a single leaf exposed to the freezing conditions which can occur in its natural environment. If this leaf is to be kept from freezing the amount of heat it loses to its surroundings must be replaced by the sprinkled water. Thus it is necessary to derive a prediction equation for the required water application rate (termed w). The development that follows will be directed toward developing a prediction equation for the theoretical application rate.

The rate at which water must be applied to the leaf surface may be postulated as a function of several independent variables.

U_a - velocity of the air

T_a - temperature of the air

RH - relative humidity of the air

f - frequency of water application

d - drop size

T_s - average temperature of the leaf surface

t - time

θ - angle of incidence

q_r - rate of heat loss by radiation

L - length of the leaf measured in the direction of air flow

i - rate of ice formation

ΔT_w - difference in the mean temperature of the water striking the leaf surface and leaving the leaf surface.

Or this may be expressed as:

$$w = w(U_a, T_a, RH, f, d, T_s, t, \theta, q_r, L, i, \Delta T_w) \qquad (3.1.1)$$

The following simplifying assumptions will be made. The drop size will be constant or at least restricted to a narrow range of values. The angle of incidence of the leaf surface will be held at zero (leaf surface parallel to the direction of air flow). Radiant heat exchange is negligible ($q_r <$ 10 percent of q_{total}). The frequency of water application will be continuous. Only steady-state conditions will be considered. The ice load will be kept at zero by employing only the sensible heat of the water (admittedly not a practical approach from the field standpoint since this will necessitate very high application rates). With these conditions imposed, the water application rate becomes a function of only six independent variables.

$$w = w(U_a, T_a, T_s, Rh, \Delta T_w, L) \qquad (3.1.2)$$

In order to determine the relationship between these six independent variables a heat balance is made on the leaf surface:

Heat added through sprinkling = total heat removed by convection + heat removed by mass-transfer,

or $$q_w = q_{ct} + q_m \qquad (3.1.3)$$

The quantity of heat added through sprinkling can be computed by the relation

$$q_w = w_t\,(5.20)\;Cp\Delta T_w \qquad (3.1.4)$$

where the constant 5.20 converts w from lb_m/min to in./min.

To obtain prediction equations for convection and mass-transfer it is necessary to assume that the leaf can be represented geometrically by a thin flat plate. Gates and Benedict (1963), found, by the use of schlieren photography that the actual measured values for heat loss by free-convection from a broad leaf compared closely with those values predicted using heat transfer theory for thin heated plates.

3.2 Convection

The rate of heat transfer from the plate surface to the moving air stream can be computed from the relation

$$q_c = \bar{h}_c\,(T_s - T_a) \qquad (3.2.1)$$

This equation has been used for many years even though it is a definition of $\bar{h}_c$ rather than a phenomenological law of convection. The equation for $\bar{h}_c$ in the case of forced convection in laminar flow over a flat plate heated over its entire length and with a constant surface

temperature is given by Kreith (1958) as

$$\bar{h}_c = .664 \frac{k}{L} Re_L^{1/2} Pr^{1/3} \qquad (3.2.2)$$

or expressed in a dimensionless term called the Nusselt number, the relation becomes

$$\overline{Nu} = \frac{\bar{h}_c L}{k} = .664 Re_L^{1/2} Pr^{1/3} \qquad (3.2.3)$$

Combining these equations the equation

$$q_c = .664 \frac{k}{L} Re_L^{1/2} Pr^{1/3} (T_s - T_a) \qquad (3.2.4)$$

represents the convective heat transfer prediction equation for heat loss from one side of the plate.

All fluid property values in equation (3.2.4) and all subsequent heat transfer equations which are dependent on temperature must be introduced at a mean temperature. The mean temperature may be calculated from the equation

$$T_m = \frac{T_s + T_a}{2}$$

Many investigators have observed that the leading edge of the leaf freezes first. On the basis of this it would be well to consider the equation for $\bar{h}_c$ for the case of a continuously varying plate surface temperature (or constant surface heat flux). The derivation of this equation follows:

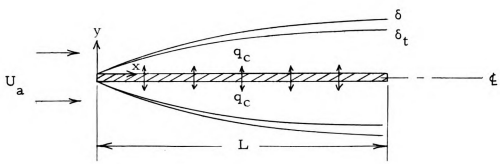

Figure 1.--Flow boundary layer and thermal boundary layer on a flat plate heated over its entire surface

The calculations are confined to a steady state, two-dimensional problem, with constant-property fluid, and velocities which are sufficiently small so that temperature increases caused in the boundary layer by internal friction can be neglected.

Since symmetry exists about the center line of the plate the derivation will be carried out for the upper plate surface. The hydrodynamic boundary layer and the temperature boundary layer begin at the leading edge of the plate since the plate is heated over its entire length. Both increase their thickness δ and δ_t in the direction of flow. Four boundary conditions can be stated.

1. at $y = 0$ $\qquad q_c = -k \frac{\partial T}{\partial y}$

2. at $y = \delta_t$ $\qquad T = T_a$

3. at $y = \delta_t$ $\quad \frac{\partial T}{\partial y} = 0$

4. at $y = 0$ $\quad \frac{\partial^2 T}{\partial y^2} = 0$

With these four conditions a polynomial with four functions will be used to express the temperature profile in the boundary layer.

$$T = A + By + Cy^2 + Dy^3$$

Using the four boundary conditions the coefficients A, B, C, and D can be determined. From boundary condition 4.

$$\frac{\partial^2 T}{\partial y^2} = 2C + 6Dy = 0 \qquad \text{but } Dy = 0 \quad \therefore \quad C = 0$$

From boundary condition 1.

$$\frac{\partial T}{\partial y} = B + 3Dy^2 = -\frac{q_c}{k} \qquad \text{but } Dy^2 = 0 \quad \therefore \quad B = -\frac{q_c}{k}$$

From boundary condition 3.

$$\frac{\partial T}{\partial y} = -\frac{q_c}{k} + 3Dy^2 = 0 \qquad \text{but } y^2 = \delta_t^2 \quad \therefore \quad D = \frac{q_c}{3k\delta_t^2}$$

From boundary condition 2.

$$A = T_a + \frac{q_c \delta_t}{k} - \frac{q_c \delta_t}{3k}$$

The equation for the temperature is

$$T = T_a + \frac{2}{3}\frac{q_c \delta_t}{k} - \frac{q_c y}{k} + \frac{q_c y^3}{3k \delta_t^2}$$

From Eckert and Drake (1959) the integral heat-flow equation of the boundary layer is

$$\frac{d}{dx}\int_o^1 (T_a - T)\, u\, dy = \alpha \left(\frac{\partial T}{\partial y}\right) y = 0 \qquad (3.2.5)$$

The integral in this equation can now be evaluated.

$$\int_o^1 (T_a - T)\, u dy = \int_o^{\delta_t} \left[-\frac{2}{3}\frac{q_c \delta_t}{k} + \frac{q_c y}{k} - \frac{q_c y^3}{3k \delta_t^2} \right] [u]\, dy$$

$$= \frac{q_c \delta_t^2 U_a}{k} \int_o^{\delta_t} \left[-\frac{2}{3} + \frac{y}{\delta_t} - \frac{y^3}{3\delta_t^3} \right]$$

$$\left[\frac{3Y}{2\delta} - \frac{1}{2}\frac{y}{\delta}^3 \right] dy$$

Now the ratios $\zeta = \delta_t/\delta$ where δ_t/δ is assumed to be less than one and $\eta = y/\delta_t$ can be introduced.

$$\int_o^1 (T_a - T)\, u\, dy = \frac{q_c\, \delta_t^2\, U_a}{k} \int_o^1 \left[-\frac{2}{3}\eta - \frac{1}{3}\eta^3 \right]$$

$$\left[\frac{3}{2}\eta\delta - \frac{1}{2}\eta^3\zeta^3 \right] d\eta$$

$$= \frac{U_a\, q_c\, \delta_t^2}{k} \left(-0.100\zeta + 0.007\zeta^3 \right)$$

Since ζ was assumed to be less than one, the second term in the right hand expression is small compared to the first and can be neglected. Introducing the value of the integral into the heat-flow equation one obtains

$$\frac{d}{dx}\left[-\frac{U_a\, q_c\, \delta_t^2}{k} \right] (0.100\zeta) = -\frac{\alpha q_c}{k}$$

Integrating this expression with respect to **x**

$$0.10\, \zeta^3\, \delta^2 = \frac{x}{U_a} + C$$

Since the plate is heated over its entire length at $x = 0$

$$\delta = 0 \quad \therefore \quad C = 0$$

$$\zeta = \left[\frac{10x}{\delta^2 U_a} \right]^{1/3} \qquad (3.2.6)$$

The integral solution given by Eckert and Drake (1959) for the hydrodynamic boundary layer thickness δ is

$$\delta = \frac{4.64x}{Re_x^{1/2}} \tag{3.2.7}$$

also

$$Re_x = \frac{U_a \times \rho}{\mu}$$

and

$$\alpha = \frac{k}{\rho Cp}$$

Introducing these expressions into equation (3.2.6) and simplifying yields

$$\zeta = \frac{1}{(1.29)\ Pr^{1/3}} \tag{3.2.8}$$

The heat flow from the plate per unit area is given by

$$q_c = -k\left(\frac{\partial T}{\partial y}\right) \quad y = 0 \tag{3.2.9}$$

or by the expression

$$q_c = h_c\ (T_s - T_a) \tag{3.2.10}$$

Equating these two expressions gives

$$h_c = \frac{3}{2} \frac{k}{\zeta\delta} \tag{3.2.11}$$

Substituting equation (3.2.8) into equation (3.2.11) gives

$$h_c = .417 \frac{k}{x} \mathrm{Re}_x^{1/2} \mathrm{Pr}^{1/3} \tag{3.2.12}$$

The average coefficient of convection given by Kreith (1958) is

$$\bar{h}_c = \frac{1}{x} \int_0^x h \, dx = 2h$$

$$\bar{h}_c' = .834 \frac{k}{L} \mathrm{Re}_L^{1/2} \mathrm{Pr}^{1/3} \tag{3.2.13}$$

or expressed in terms of the dimensionless Nusselt number

$$\overline{Nu} = \frac{\bar{h}_c' L}{k} \tag{3.2.14}$$

The prime designation on the coefficient of convection term will be used to distinguish it from the coefficient of convection term for the case of a flat plate with a constant surface temperature. Equation (3.2.13) indicates that the rate of heat removal from a plate whose surface temperature is continuously varying is 25.6 percent greater than that obtained from a plate whose surface temperature is constant. The quantity of heat removed per unit time per unit area for a plate

with a continuously varying surface temperature is given by the relationship

$$q_c' = \bar{h}_c' \ (T_p - T_a) \tag{3.2.15}$$

The temperature T_p is obtained by plotting the temperature profile curve (local plate surface temperature versus distance from the leading edge), finding the area under the curve, and obtaining the temperature which divides this area in half.

An alternate solution [Eckert and Drake (1959)] for obtaining the local heat flux from a flat plate with a continuously varying surface temperature involves integration of the equation

$$q = \int_o^x h(x, \xi) \ dt_p \ (\xi)$$

where dt_p is interpreted as a succession of infinitesimally small temperature steps occurring at infinitesimally closely spaced locations $d\xi$. In view of the fact that the evaluation of this equation is rather tedious an approximate equation offered by Eckert and Drake (1959) can be used. The approximate equation, which by actual test deviates only a few percent from the exact solution, for the total heat flux with laminar air flow is

$$q_c' = \bar{h}_c \left\{ \Delta t_o + .969 \ (\Delta t_n - \Delta t_o) - .432 \ \frac{\Delta L}{L} \right.$$
$$\left. \left[(2n - 1) \ \Delta t_n - \Delta t_o - 2 \sum_{n=o}^{n} \Delta t_n \right] \right\} \tag{3.2.16}$$

where $\bar{h}_c$ is the average coefficient of convection for a plate with a constant surface temperature defined by equation (3.2.2). Δt and ΔL are explained in the following figure;

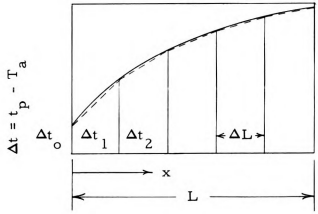

Figure 2.--Approximation of continuously varying wall temperature by straight line segments.

Letting $\Delta T_p'$ equal the quantity within the outer brackets of equation (3.2.16) the equation can be written as

$$q_c' = \bar{h}_c \Delta T_p'$$

3.3 Mass-Transfer

Water vapor is transferred from any water film on the leaf surface to the air by the process of evaporation or mass-transfer. For every pound of water removed by this process 1070 Btu's of heat are required (for water at 32 F). To arrive at a prediction equation for this heat loss use is made of the similarity relations between

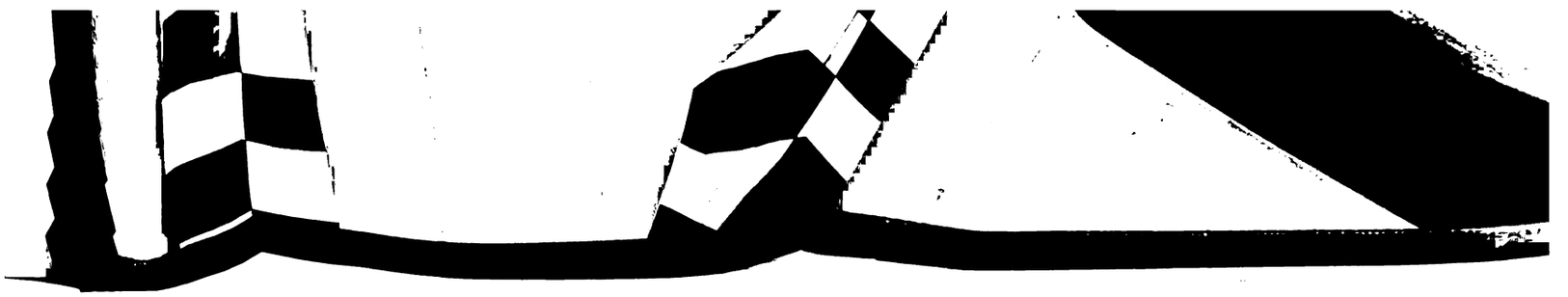

heat and mass-transfer. The following assumptions are made:

1. The fluid properties are approximately constant.

2. The temperature differences in the field are small when compared to the absolute temperature.

3. The pressure is approximately constant.

When these assumptions are met then any of the equations for heat transfer in laminar flow also gives the solution for a corresponding mass-transfer problem if the Nusselt number $\frac{\bar{h}_c L}{k}$ is replaced by the dimensionless mass-transfer coefficient $\frac{\bar{h}_m L}{D}$ and the Prandtl number (ν/α) by the Schmidt number (ν/D). The rate of mass transfer can then be given as

$$m_s = \frac{\bar{h}_m}{R T} (P_s - P_a) \qquad (3.3.1)$$

where P_s is the saturated vapor pressure at the water surface and P_a is the vapor pressure of the air.

The validity of the similarity relations has been proven by many investigators. Hartnett and Eckert (1957) determined the temperature and concentration profiles in a laminar boundary layer on a flat plate. Their investigations show that the mass-fraction and the temperature profiles are similar when Pr = Sc or when the ratio Sc/Pr = α/D, called the Lewis Number, is 1. For water diffusing into air at 46.4 F the Lewis Number is 0.85.

The average mass-transfer coefficient for laminar flow over a water surface with a constant surface temperature is given by the relation

$$\bar{h}_m = .664 \frac{D}{L} Re_L^{1/2} Sc^{1/3} \quad (3.3.2)$$

$\bar{h}_m$ can also be expressed by an average dimensionless mass-transfer number analogous to the Nusselt number for convective heat transfer.

$$\overline{Nm} = \frac{\bar{h}_m L}{D} \quad (3.3.4)$$

The quantity of heat loss through the mass-transfer process can then be computed from the relation

$$q_m = H_v m_s \quad (3.3.5)$$

Upon substituting the equations for m_s and $\bar{h}_m$ the final form of the prediction equation becomes

$$q_m = (.664) \frac{H_v D}{R T L} Re_L^{1/2} Sc^{1/3} (P_s - P_a) \quad (3.3.6)$$

3.4 Sprinkling the Leaf Model

The quantity of water used for cold protection must be such that it will supply enough sensible heat to compensate for the heat loss by convection and mass-transfer. In actual field practice,

this approach is impractical. For every pound of water that freezes on the leaf there is released 144 Btu's of heat. If there were a ten degree difference between the mean temperature of the water striking the leaf and the mean temperature of the water leaving the leaf it would require 14.4 times more water to protect the leaf using only the sensible heat. However, this approach will be taken (employment of sensible heat only) in order to facilitate an accurate basic analysis of the heat transfer phenomena taking place on the leaf model.

The leaf will lose sensible heat by forced convection from both its upper and lower surfaces. Heat loss due to mass-transfer will occur only from those areas of the leaf covered with a water film. In its natural state it is possible for a leaf with a hydrophobic surface to have neither side completely covered with a water film. Instead the water may bead-up in the form of droplets scattered over the surface. In this study of the leaf model it is assumed that a continuous water film exists over the entire upper surface only. Heat is removed from this water film surface by convection, equation (3.2.1) and by mass-transfer, equation (3.3.5). Occurring simultaneously with the above mentioned heat losses is the convective loss from the underside of the leaf model in accordance with equation (3.2.17). Combining these two convective losses the total heat removed by convection is defined as

$$q_{ct} = \bar{h}_c' \, \Delta T_p' + \bar{h}_c \, (T_s - T_a) \qquad (3.4.1)$$

Substitution of equations (3.1.4), (3.4.1), and (3.3.6) for the three terms in the heat balance equation (3.1.3) gives the following relationship;

$$5.2\, w_t\, Cp\, \Delta Tw = .664\, \frac{k}{L}\, Re_L^{1/2}\, Pr^{1/3}\, \Delta T_p' + .664\, \frac{k}{L}\, Re_L^{1/2}\, Pr^{1/3}\, (T_s - T_a) + \frac{H_v\, D}{R\, T\, L}\, Re_L^{1/2}\, Sc^{1/3}\, (P_s - P_a)$$

Simplifying and rearranging terms the prediction equation for the water application rate is

$$w_t = \frac{Re_L^{1/2}}{5.2L\, Cp\, \Delta T_w} \left[.664\, k\, Pr^{1/3}\, \Delta T_p' + .664\, k\, Pr^{1/3}\, (T_s - T_a) + \frac{H_v\, D}{R\, T}\, Sc^{1/3}\, (P_s - P_a) \right] \qquad (3.4.2)$$

Inspection of this equation reveals that the water application rate is indeed a function of the six independent variables set forth in relationship (3.1.2). To correlate these six independent variables with respect to the dependent variable w it is necessary to derive a dimensionless water application rate number which can

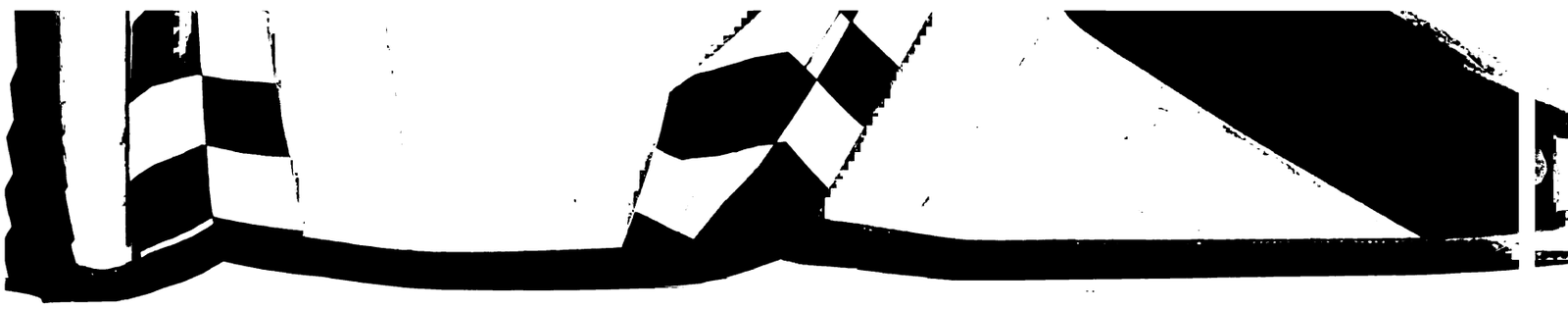

be plotted against the Reynolds number. The equation defining the dimensionless water application rate number is

$$W = \frac{5.20\, w_t\, Cp\, \Delta T_w}{q_c' + q_c + q_m} \qquad (3.4.3)$$

If the expressions for the three terms in the denominator of this equation, along with their respective film-transfer coefficients, are introduced the equation takes the form

$$W = \frac{5.20\, w_t\, Cp\, \Delta T_w\, L}{\overline{Nu'}\, k'\, T_p' + \overline{Nu}\, k(T_s - T_a) + \dfrac{\overline{Nm}\, H_v\, D\, (P_s - P_a)}{R\, T}} \qquad (3.4.4)$$

$\overline{Nu'}$ will be obtained experimentally in the ensuing study and may differ somewhat from equation (3.2.14). This difference, if it occurs will, in all probability, be in the constant of the average film heat transfer coefficient.

be plotted against the Nusselt number. The equation defining the dimensionless water evaporation rate number is

$$W = \frac{\dot{m}_w}{\pi \rho_a^2 \nu_a^2} \qquad (3.4.3)$$

If the exponents for the Prandtl number in the denominator of this equation, along with their respective film-transfer coefficients, are introduced the equation becomes

$$W = \frac{\dot{m}_w}{\overline{Nu}\, \pi \rho_a^2 \nu_a^2 + \overline{Nu}\, \pi (T_s^3 + T_a^3) + \overline{Nu}\, \pi D (P_s^3 - P_a^3)} \qquad (3.4.4)$$

$\overline{Nu}$ will be obtained experimentally in the ensuing study and may differ somewhat from equation (3.2.14). This difference, if it occurs will, in all probability, be in the constant of the average film heat transfer coefficient.

IV. EXPERIMENTAL EQUIPMENT

4.1 Wind Tunnel

A wind tunnel was constructed to provide an environment for the leaf model where the independent variables air velocity, temperature, and relative humidity could be controlled, and also an environment in which radiant heat exchange was eliminated. The desired range of each of the independent variables (selected on the basis of actual field conditions) of air velocity, temperature, and relative humidity was, respectively, 50 to 900 ft/min, 15 to 32 F, and 25 to 100 percent.

A tunnel (Figure 3) 10 ft long with inside dimensions of 11 in. x 12 in. was constructed from 3/8 in. plywood and lined inside with 2 in. thick Styrofoam. The tunnel was equipped with two access doors, one in the inlet section, the other in the downstream test area. The access door in the test area was fitted with a plastic window to permit visual observation of the experimental equipment during testing.

To reduce free stream turbulence and produce a uniform velocity profile in the tunnel cross section the following equipment was arranged in the inlet section (initial five feet) of the tunnel

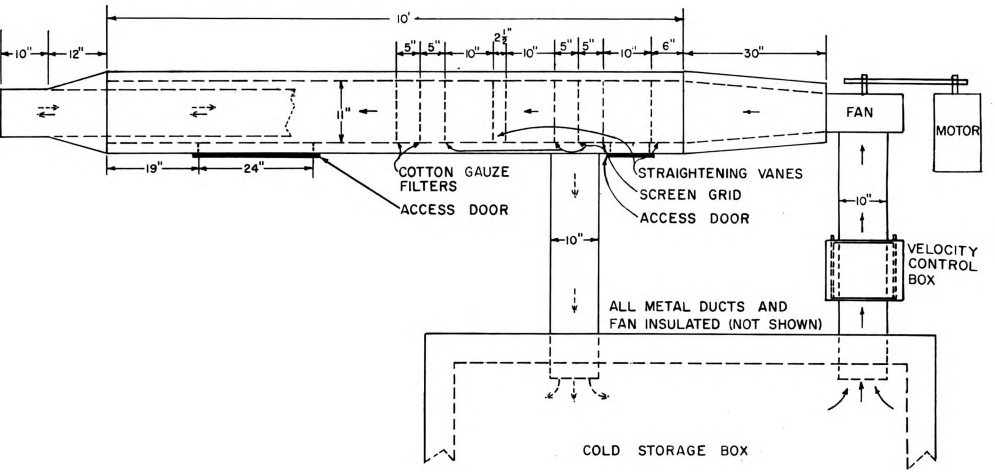

Figure 3.--Wind tunnel layout.

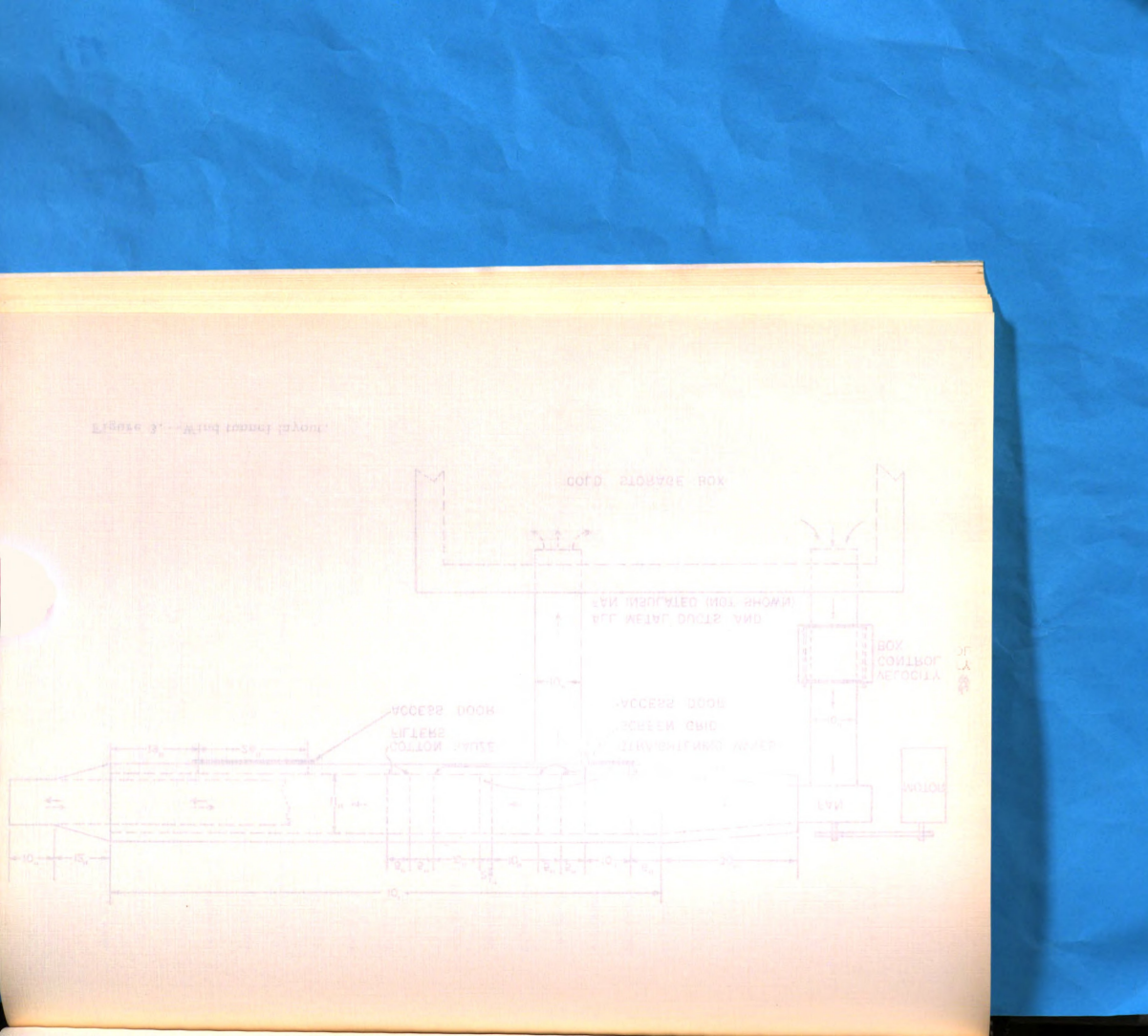

(Figure 4). Located in the tunnel entrance was a set of 2 in. diameter straightening vanes 6 in. in length. Following this were three screen grids, a second set of straightening vanes 3/16 in. in diameter by 2 1/2 in. in length (constructed from plastic straws), a fourth screen grid, and finally two cotton gauze filters. The top of the tunnel was constructed so that it could be removed in two separate sections to facilitate placement of the straightening vanes, grids, and filters.

The cold air supply was obtained from a 650 cu ft cold storage box with an approximate net cooling capacity of 12,000 Btu/hr. The cold storage refrigeration unit could be set to maintain a desired temperature within ± 2.0 degrees Fahrenheit. The air was brought to the fan intake via the velocity control box through a 10 in. diameter metal duct wrapped with a 4 in. thick batting of fiberglass insulation. The cold air leaving the tunnel was returned to the cold storage box by a similarly constructed duct system.

4.1.1 Temperature

The air temperature in the test area of the tunnel was measured with two thermocouples located 1 ft upstream from the test area and 5 1/2 in. above the tunnel floor (centered vertically). The thermocouples were made of 30 gage copper-constantan wire insulated with enamel and glass. These thermocouples have an accuracy of approximately ± 3/4 percent of the standard emf temperature

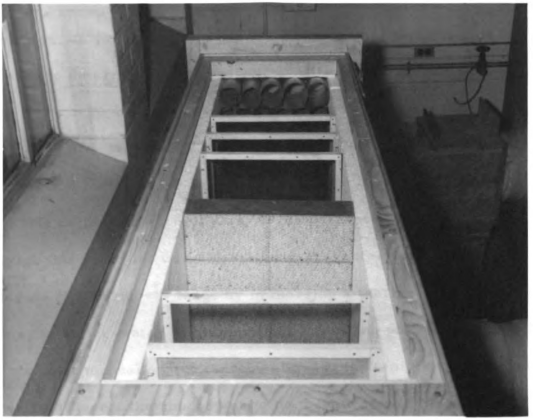

Figure 4.--Inlet section of wind tunnel.

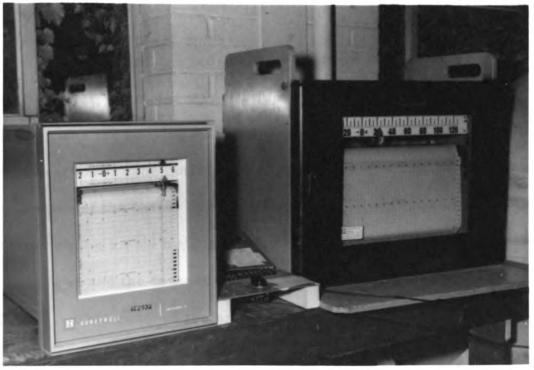

Figure 5.--Temperature recording potentiometers.

calibration. A Honeywell two pen strip chart recorder (Figure 5) was used to determine the temperature indicated by the emf output of the thermocouples. The temperature range of the recorder was from -20 to +60 degrees Fahrenheit. It was possible to read the chart scale directly to 1.0 degree and estimate it to 0.1 of a degree. Full scale calibrated accuracy was ± .25 percent of instrument span. Although this recorder was calibrated at the factory a check at the 32 degree F reading was made by immersing a thermocouple junction in an agitated ice-water mixture. Each recording pen was connected to a six point manual switch thereby allowing the temperatures sensed by twelve different thermocouples to be measured and recorded.

4.1.2 Velocity

A forward-curved-blade centrifugal fan driven by a single phase 5 hp electric motor was used to provide the required air velocity. The fan housing was wrapped with fiberglass insulation to reduce heat loss. The outlet section of the fan was connected to the inlet section of the tunnel by means of a tapered plywood conduit insulated on the inside by 2 in. of Styrofoam. The connection between the fan outlet and the tapered conduit was made with a flexible piece of canvas. This reduced the amount of vibration transmitted from the fan to the tunnel.

Velocity control was made possible by a sliding door arrangement located in the intake duct. Movement of the door simply increased or decreased the effective size of the fan intake opening thereby increasing or decreasing the air velocity.

The time-averaged velocity of air movement in the tunnel was measured with a constant current hot-wire anemometer (Figure 6); model HWB ser. no. 216 by Flow Corporation. The hot-wire probe was a standard 24 in. Flow Corporation probe fitted with a tungsten filament 0.0625 in. long and 0.0005 in. in diameter. The probe sensing element (filament) was located approximately two feet upstream from the test area and in the center of the tunnel cross section. The hot-wire anemometer was calibrated against a pitot tube installed in the tunnel. The pressure head difference from the pitot tube was sensed by an inclined manometer filled with a fluid of .797 specific gravity. The scale on the manometer could be read to .005 in. For the pitot tube used, the velocity was determined by the equation

$$U_a = 66.75 \quad h^{1/2} \qquad (4.1.2.1)$$

where h is the manometer reading in in. and U_a the velocity in ft/sec. Velocity measurements with the hot-wire anemometer were considered to have an accuracy of ± 2.0 percent.

4.1.3 Turbulence

The degree of free stream turbulence was investigated by using the hot-wire anemometer described in section 4.1.2. The signal from the hot-wire anemometer amplifier was fed through a 7KC low pass filter to a true root-mean-square voltmeter (Figure 6); Model No. 320 by Ballantine Laboratories. An oscilloscope was used to obtain the correct square-wave compensation frequency setting for the hot-wire anemometer amplifier. Detailed operating instructions for obtaining the average velocity and degree of turbulence are given in Flow Corporation Bulletin No. 37B.

4.1.4 Relative humidity

The humidity in the closed air system for the tunnel was not controlled. Since a measure of the relative humidity at any time was obtainable it was felt that the difficulties (air temperatures below freezing) and cost accompanying the installation of a humidity control system could not be justified in this study.

The relative humidity of the air in the wind tunnel was determined with a Honeywell Model w611A Portable Relative Humidity Indicator (Figure 7). Seven lithium chloride humidity sensors were available as plug-in components for the probe assembly, each designed for a specific RH range. By a simple change of sensing unit and indicator scale plate relative humidities ranging from 2 to 100

4.1.3 Turbulence

The degree of free stream turbulence was investigated by using the hot-wire anemometer described in section 4.1.2. The signal from the hot-wire anemometer unit was fed through a TKC low pass filter to a true root mean square voltmeter (Flystr of: Model No. 320 by Hastings Instruments). An oscilloscope was used to obtain the rotest square wave response/oscillation frequency setting for the hotwire anemometer amplifier. Operating instructions for obtaining the average working the degree of turbulence are given in Flow Corporation Bulletin No. 118.

4.1.4 Relative humidity

The humidity in the closed air system for the tunnel was not controlled. Since a measure of the relative humidity at any time was obtainable it was felt that the difficulties (air temperatures below freezing) and cost accompanying the installation of a humidity control system could not be justified in this study.

The relative humidity of the air in the wind tunnel was determined with a Honeywell Model 9611A Portable Relative Humidity Indicator (Figure 7). Seven lithium chloride humidity sensors were available as plug-in components for the probe assembly, each designed for a specific RH range. By a simple change of sensing unit and indicator scale plate relative humidities ranging from 2 to 100

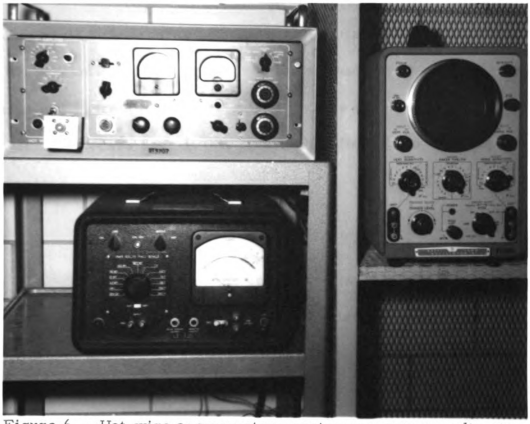

Figure 6.--Hot-wire anemometer, root-mean-square voltmeter, and oscilloscope.

Figure 7.--Relative humidity indicator and sensors.

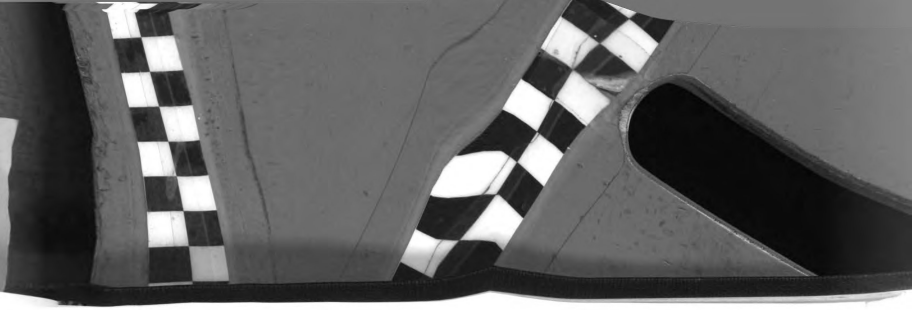

percent could be measured. The over-all instrument accuracy was ± 3 RH percent. The probe to which the sensors were attached was located just in front of the straightening vanes at the entrance to the tunnel. The access door at this location facilitated the changing of the sensors.

4.2 Heated Flat Plate

The evaluation of the convective (sensible) heat loss under the simulated air temperatures and velocities experienced in the field was made using a heated flat plate.

The heated plate used in this study was constructed from two pieces of aluminum each having a thickness of .051 in. The top section of the 6 in. x 6 in. plate (Figure 8) was provided with .35 in. x .35 in. tabs for mounting on the test stand. The inside surface of each piece of aluminum was sprayed with two coats of Krylon-red insulating varnish forming a thin die-electric layer. Number 32 bare Nickle Chromium wire was laid out over the entire surface a distance of .25 in. apart and sprayed into place with an additional coat of insulating varnish. This arrangement produced a resistance heating element with a total resistance of 112 ohms. Plate surface temperatures were sensed by means of five thermocouples mounted flush with the surface. The exact locations are shown in Figure 8. The thermocouple junctions were made from number 30 copper-constantan wire. These junctions were forced through a 0.023 in.

percent could be measured. The over all instrument accuracy was ± 3 RH percent. The [illegible] to which the sensors were attached was located just in front of the [illegible] at the entrance to the tunnel. The access [illegible] facilitated the changing of the sensors.

[illegible] Flat Plate

The [illegible] heat loss under the simulated [illegible] temperatures and velocities experienced in the field was made [illegible] flat plate.

The [illegible] plate used in this study was constructed from two pieces of aluminum [illegible] having a thickness of .051 in. The top section of the 6 in. x [illegible] plate (Figure 8) was provided with .35 in. x .35 in. tabs for mounting on the test stand. The inside surface of each piece of aluminum was sprayed with two coats of Krylon-red insulating varnish forming a thin die-electric layer. Number 32 bare Nickle Chromium wire was laid out over the entire surface a distance of .25 in. apart and sprayed into place with an additional coat of insulating varnish. This arrangement produced a resistance heating element with a total resistance of 112 ohms. Plate surface temperatures were sensed by means of five thermocouples mounted flush with the surface. The exact locations are shown in Figure 8. The thermocouple junctions were made from number 30 copper-constantan wire. These junctions were forced through a 0.023 in.

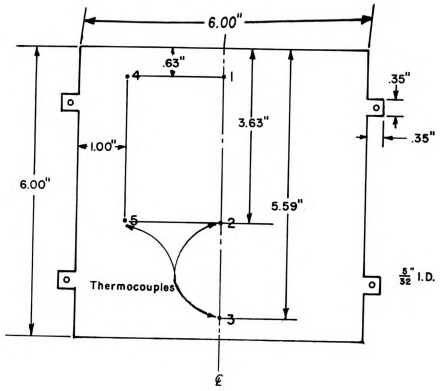

TOP VIEW

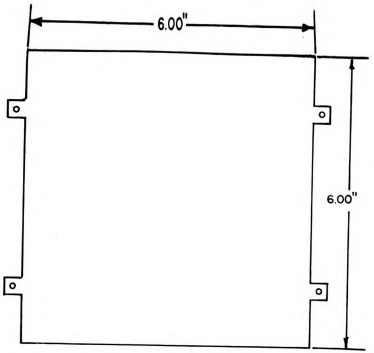

BOTTOM VIEW

END VIEW

Figure 8. --Dimensional view of heated flat plate.

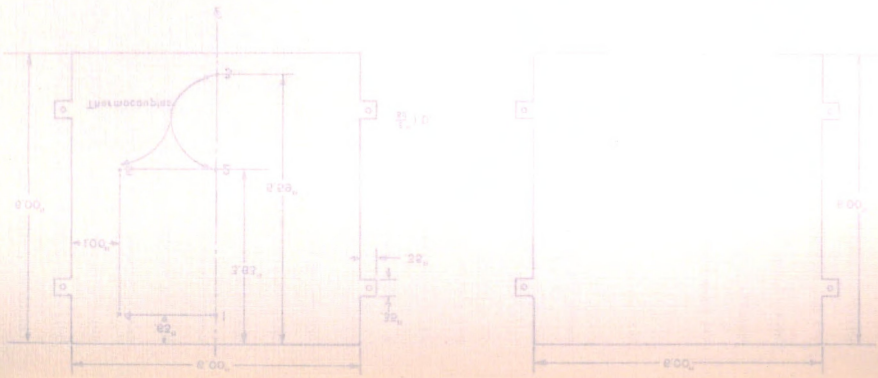
END VIEW
TOP VIEW
BOTTOM VIEW
Thermocouple

diameter hole and fitted flush with the top surface. Care was taken to position the thermocouple lead wires between the heating wires on the inside plate surface. Since the boundary layer development for the top of the plate is analogus to that for the bottom, no thermocouples were installed in the bottom surface of the plate.

Following installation of the five thermocouple junctions, the two halves of the plate were pressed together and cemented in place with Corona Dope (a high voltage insulating material). The completed plate (Figure 9) with an overall thickness of 0.125 in. was then sprayed with a single coat of insulating varnish to provide a uniform finish on the upper and lower surfaces.

Two variable DC power supply units with a maximum output of 500 volts and 200 milliamperes were connected in parallel to provide the current for the heating element in the plate. Two Weston analyzers were employed for measuring the voltage and current supplied to the heating element. These units were calibrated against a standard power supply unit accurate to ± 0.2 percent.

The plate was mounted on a test stand (Figure 10) by means of small plastic tabs which were attached to the tabs provided on the top half of the plate. The test stand was constructed so that it was possible to raise or lower any corner of the plate. This provided a means for adjusting the plate surface attitude with respect to the direction of air travel in the tunnel. The plate and the test stand

diameter hole and [illegible] was taken
to position the [illegible] the heating wires on
the inside plate [illegible] development for
the top of the pla[illegible] the thermocouples
were installed [illegible].

[illegible] couple junctions, the
two halves of [illegible] cemented in place
with Corona D[illegible]. The completed
plate (Figure 9) [illegible] was then sprayed
with a single [illegible] provide a uniform finish on
the upper and lower [illegible].

Two [illegible] supply units with a maximum output of 500 volts [illegible] were connected in parallel to provide the current [illegible] heating elements in the plate. Two Weston analyzers were employed for measuring the voltage and current supplied to the heating element. These units were calibrated against a standard power supply unit accurate to ± 0.2 percent.

The plate was mounted on a test stand (Figure 10) by means of small plastic tabs which were attached to the tabs provided on the top half of the plate. The test stand was constructed so that it was possible to raise or lower any corner of the plate. This provided a means for adjusting the plate surface attitude with respect to the direction of air travel in the tunnel. The plate and the test stand

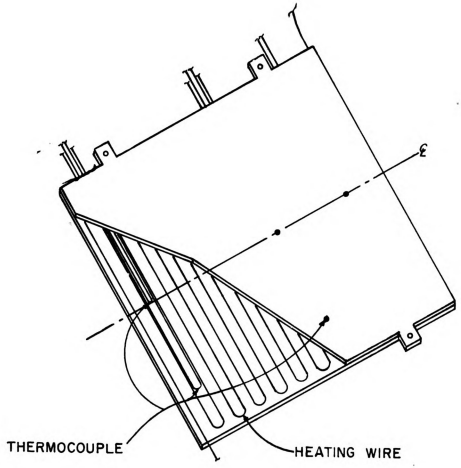

Figure 9.--Cutaway view of heated flat plate.

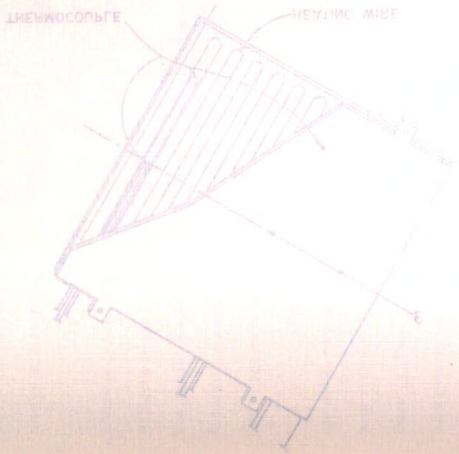
THERMOCOUPLE
HEATING WIRE

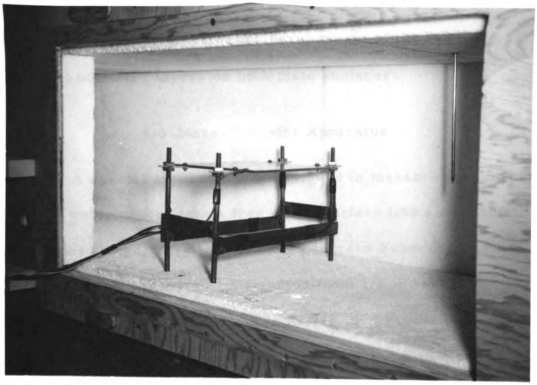

Figure 10.--Heated flat plate located in test area.

Figure 11.--Equipment set-up for measuring mass-transfer.

so designed, permitted undisturbed development of the hydrodynamic and thermal boundary layers on both plate surfaces.

4.3 Mass-Transfer Apparatus

A special apparatus was designed to measure the mass-transfer of water vapor from a free water surface into a moving air stream whose temperature was below 32 degrees Fahrenheit. The apparatus consisted of a tray constructed from 1/8 in. thick plastic with inside dimensions of 8 in. x 8 in. x 7/8 in. (Figure 12). All four sides and the bottom of the tray were insulated with a 1 in. thickness of Styrofoam. A 1/2 in. hooded water inlet was provided through the center of the tray bottom and attached to three feet of flexible plastic tubing. A plastic grid made of 1/8 in. plastic, 3/10 in. deep was installed flush with the tray surface dividing the surface area into 9 equal parts. The purpose of the grid was to provide support for the porous cotton cloth which was stretched across the tray surface. Thermocouple junctions were threaded into the cloth surface at selected locations (Figure 12) and sewed in place. These thermocouples measured the temperature of the water surface. The thermocouple lead wires were located beneath the cloth surface. To keep the water surface from freezing during the test runs, a plastic coated nickel-chromium heating wire was arranged at 1/2 in. intervals over the bottom of the tray (Figure 13). The resistance of this heating wire was approximately 7 ohms per foot. One end of the heating wire

so designed, permitted controlled flow of steam of the hydrodynamic and thermal boundary layers can be given patterns.

A type of [illegible] was designed to measure the mass- transfer of water [illegible] into a moving air stream whose temperature [illegible] throughout. The apparatus consisting of [illegible] thick plastic with inside dimensions of [illegible] (Figure 12). All four sides and the top of the tray were machined with a 1 in. thickness of Styrofoam. A 1/2 in. inverted water inlet was provided through the center of the tray bottom and attached to three feet of flexible plastic tubing. A plastic grid made of 1/8 in. plastic, 3/10 in. deep was installed flush with the tray surface dividing the surface area into 9 equal parts. The purpose of the grid was to provide support for the porous cotton cloth which was stretched across the tray surface. Thermocouple junctions were threaded into the cloth surface at selected locations (Figure 12) and sewed in place. These thermocouples measured the temperature of the water surface. The thermocouple lead wires were located beneath the cloth surface. To keep the water surface from freezing during the test runs, a plastic coated nickel-chromium heating wire was arranged at 1/2 in. intervals over the bottom of the tray (Figure 13). The resistance of this heating wire was approximately 7 ohms per foot. One end of the heating wire

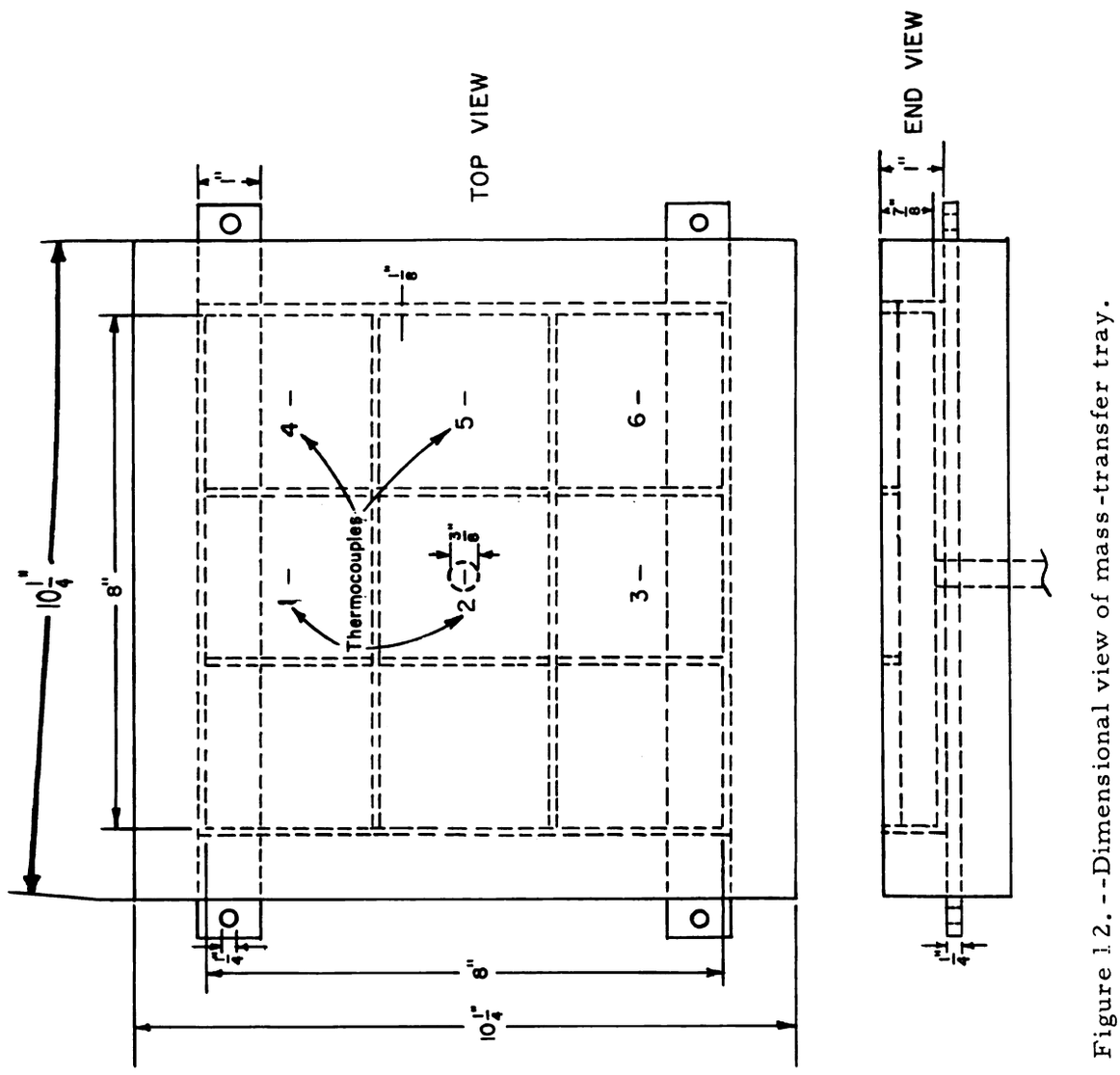

Figure 12.--Dimensional view of mass-transfer tray.

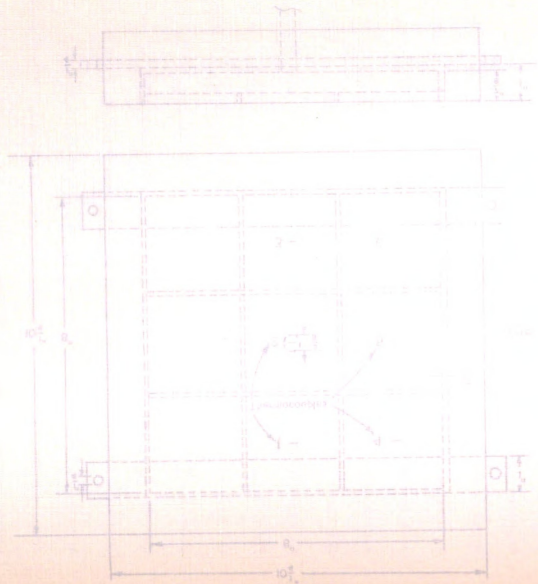
END VIEW

HEATING WIRE

was wound around the exposed (to the tunnel air) plastic tubing leading from the tray bottom to the outside of the tunnel and insulated to prevent freezing of the water therein. Plastic cement was used to seal the cloth to the top edge of the tray in order to insure that mass-transfer would take place only from the 8 in. x 8 in. tray surface.

A similar 8 in. x 8 in. 7/8 in. tray of 1/8 in. plastic was constructed for the purpose of providing a constant-head water reservoir for the test tray in the tunnel (Figure 11). This tray was covered with the exception of a small access hole, to prevent evaporation of the water. The tray was not insulated since it was only subject to the ambient temperature outside the tunnel. The tray bottom was fashioned so that it would rest securely on the head of a balance. This arrangement provided a constant-level support and a means of measuring the amount of water removed from the tray (to replenish the water lost by mass-transfer from the tray surface in the tunnel). A Mettler Balance with a capacity of 800 grams which could be read directly to 0.1 gram and estimated to 0.01 gram was used.

To provide the required DC current to the heating wire in the test tray three variable DC power supply units were used. Each of these units had a maximum capacity of 500 volts and 200 milliamperes. When these units were connected in parallel a maximum of 600 milliamperes of DC current was available for the heating wire.

was wound around the exposed [illegible] plastic tubing lead-
ing from the tray bottom to the outside of the tunnel and insulated to
prevent freezing of the water [illegible] was used to
seal the cloth to the [illegible] to insure that mass-
transfer would take [illegible] tray surface.

A similar [illegible] plastic
was constructed for the [illegible] constant-head water
reservoir for the [illegible]. This tray was
covered with the [illegible] hole, to prevent evapora-
tion of the water. The tray was not insulated since it was only subject
to the ambient temperature outside the tunnel. The tray bottom was
fashioned so that it would rest securely on the head of a balance. This
arrangement provided a constant-level support and a means of measur-
ing the amount of water removed from the tray (to replenish the water
lost by mass-transfer from the tray surface in the tunnel). A Mettler
Balance with a capacity of 800 grams which could be read directly to
0.1 gram and estimated to 0.01 gram was used.

To provide the required DC current to the heating wire in
the test tray three variable DC power supply units were used. Each
of these units had a maximum capacity of 500 volts and 200 milli-
amperes. When these units were connected in parallel a maximum of
600 milliamperes of DC current was available for the heating wire.

4.4 Leaf Model

A model of a leaf (flat plate) was constructed so that the validity of equation (3.4.2) could be examined under actual sprinkling conditions.

A 4 in. x 4 in. leaf model (Figure 14) was constructed from two pieces of .051 in. thick aluminum in the same manner as the plate described in section 4.2. Three thermocouples were located in the bottom plate surface at distances of .168 in., 1.250 in., and 3.000 in. measured from the leading edge along the center line of the plate. The plate was mounted on an adjustable stand. A plastic trough made from 1/2 in. diameter tubing was fastened to each side and the back of the plate to intercept the water leaving the plate surface. The troughs on each side of the plate were closed at the front (leading edge) and open at the back. The trough at the rear of the plate was closed at both ends with an exit located at the center. Two thermocouples were located in each of the three troughs to provide a measure of the temperature of the water as it left the plate. Each trough was covered by a sloping (away from the plate surface) plastic canopy 1/2 in. above the plane of the plate surface. The leading edge of the canopy was located directly above the edge of the plate so that it did not prevent precipitation from falling directly onto the plate itself. It did, however, prevent precipitation from falling directly into the surface water collecting troughs. The canopies were

A model of a flat roof plate was constructed so that the validity of equation 12 could be tested under actual sprinkling conditions.

A 4 in. × 4 in. [illegible] was constructed from two pieces of [illegible] in the same manner as the plate described in section 2.4. The thermocouples were located in the bottom plate [illegible] and 3.000 in. measured from the [illegible] edge along the center line of the plate. The plate was supported on an adjustable stand. A plastic trough made from 1/4 in. material long was fastened to each side and the back of the plate to intercept the water leaving the plate surface. The troughs on each side of the plate were closed at the front (leading edge) and open at the back. The trough at the rear of the plate was closed at both ends with an exit located at the center. Two thermocouples were located in each of the three troughs to provide a measure of the temperature of the water as it left the plate. Each trough was covered by a sloping (away from the plate surface) plastic canopy 1/2 in. above the plane of the plate surface. The leading edge of the canopy was located directly above the edge of the plate so that it did not prevent precipitation from falling directly onto the plate itself. It did, however, prevent precipitation from falling directly into the surface water collecting troughs. The canopies were

Figure 14.--Leaf model in test area of wind tunnel.

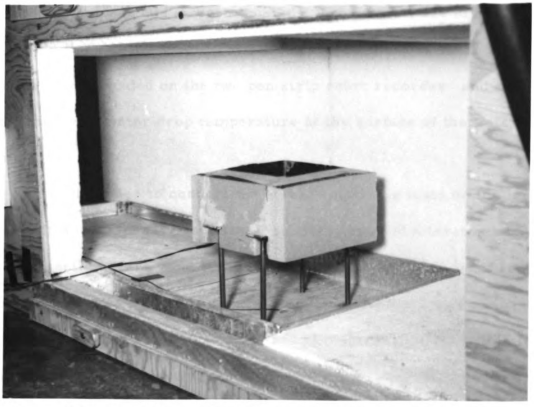

Figure 15.--Tray for measuring water application rate and drop temperature.

mounted in such a manner that there was no interference to the free development of the boundary layers over the plate surfaces. The temperature of the water film on the plate surface was measured by three thermocouples laid on top of the plate.

The water application rate and the mean temperature of the water drops striking the water surface were measured by means of a 4 in. x 4 in. x 1/2 in plastic tray (Figure 15). The tray was insulated with a one inch thickness of Styrofoam about its exterior and fitted with adjustable support legs. The top edge of the tray and insulation were sloped away from the interior edge of the opening to insure that only the precipitation from a 4 in. x 4 in. area entered the tray. The thermocouples were located approximately 1/4 in. above the inside floor of the tray. The temperature sensed by these thermocouples was recorded on the two pen strip chart recorder and indicated the mean water drop temperature at the surface of the water film.

In order to conduct the actual sprinkling tests on the leaf model, it was necessary to make some additions and alterations to the test section of the wind tunnel. Initially a 12 in. x 12 in. roof section over the test area was removed. Fitted to this opening was an insulated plywood sprinkling tower 18 1/2 in. high (Figure 16) with a full cone spray nozzle assembly installed at the top. The front section of the tower was removable thereby providing easy access to the spray

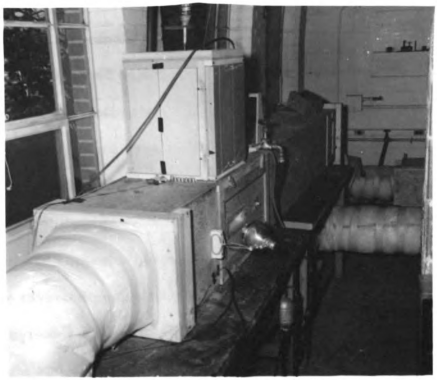

Figure 16.--Wind tunnel with sprinkling equipment attached.

Figure 17.--Sprinkling tower and water control assembly.

nozzle. The water supply and pressure to the nozzle were controlled by an assembly located adjacent to the tower (Figure 17). It was comprised of a shut-off value, diaphragm pressure regulator (0-125 $lb/in.^2$ and a pressure gage (0-100 $lb/in.^2$ Inside the tower (Figure 17) an inverted cone (made from a 6 1/2 in. diameter funnel) with a 3/4 in. diameter opening was located 2 and 3/8 in. below the spray nozzle to control the diameter of the spray pattern in the test area. The inverted cone was placed over a 4 1/2 in. diameter by 2 in. high open cylinder affixed to the center of a 12 in. x 12 in. metal pan which caught and drained-off all water not passing through the cone opening. Attached to the 4 1/2 in. opening on the under side of the pan was a 9 1/2 in. diameter cone which served to intercept and divert (away from the center of the test area) any water droplets forming about the periphery of the opening. A 12 in. x 12 in. piece of insulation was removed from the floor of the test area directly beneath the sprinkling tower. A sheet metal pan with drain was installed in its place to collect the sprinkled water. A one inch deep 16 1/2 in. long metal splash pan was installed down wind from the test area to intercept any spray carried past the collector pan. This pan was installed flush with the tunnel floor and drained forward into the collector pan in the test area. Thermocouples were attached to the spray nozzle and the drain in the collector pan to measure incoming and outgoing water temperatures respectively.

The thermocouples sensing the air temperature approaching and leaving the test area and the water temperature at the spray nozzle and in the collector pan were connected to a 16 point Brown Potentiometer (Figure 5). This recorder had a scale reading from -20 F to 120 F and could be read directly to 0.5 F. Since the recorder had a 15 second pen speed connecting 4 points in series it provided a recording of each of the four temperatures every one minute. The six thermocouples used to measure the water temperature in the collector troughs were connected to one pen of the two pen strip chart recorder through the six-position manual switch. The three thermocouples located in the bottom plate surface and the three thermocouples lying on top of the upper plate surface were connected to the second pen through a six-position manual switch.

V. EXPERIMENTAL PROCEDURE

5.1 Convection

The independent variables and their range of values studied in Phase One of the investigation were:

a. air velocity (51 to 961 ft/min)

b. air temperature (10.1 to 25.0 F)

The heat transferred from both sides of the flat plate was determined for various values of the above variables. A total of 19 tests were made.

Prior to the actual test period the cooling coils on the cold storage box refrigeration unit were defrosted, the thermostat set at 19 degrees F, and the temperature in the box allowed to come to equilibrium.

The initial step was to properly position the stand supporting the plate in the test area of the tunnel. The stand was centered horizontally and the plate adjusted until it was centered vertically making sure the plate surface was parallel with the tunnel floor. After closing the access door to the test area, the velocity control gate was fully opened and the fan started. The strip chart recorder and the DC power supply units were then turned on. The

output from the power supply units was adjusted until the plate temperature indicated by the number one thermocouple was brought to a steady-state value of approximately 31 F. Once assured that steady-state air temperature and plate temperature were reached, the values for the heating element voltage and current along with the current reading from the hot-wire anemometer were recorded. Immediately following these readings, the temperature values indicated by plate surface thermocouples two through five were recorded by manually switching to each thermocouple for a brief time interval.

The velocity control gate was then reset to provide a lower air velocity and the above procedure repeated.

5.2 Mass-Transfer

The independent variables and their range of values studied in Phase Two of the investigation were:

a. air velocity (161 to 866 ft/min)

b. air temperature (15.1 to 22.1 F)

c. relative humidity of the air (40 to 63 percent)

The mass-transfer from a free water surface was determined for various values of the above variables. A total of 6 tests were run.

The mass-transfer tray was positioned in the center of the test area and leveled by adjustment of the support legs. Before each test run the balance supporting the water-reservoir tray was calibrated with respect to water removal from the mass-transfer

tray in the tunnel. This was accomplished by bringing the water-reservoir tray to a fixed position using a device on the balance which secured the balance head for transport. Distilled water was added to the water-reservoir tray until the desired level of water was obtained in the mass-transfer tray. Following this the clamp located adjacent to the outside tunnel wall on the plastic tubing connecting the trays was closed. The positioning mechanism on the balance was released and a reading taken. The water-reservoir tray was then returned to its initial position the clamp opened and a small quantity of water removed from the mass-transfer tray. After sufficient time had elapsed for equalization of the water levels in the two trays, the clamp was closed and a second reading taken. This procedure was repeated five times and each time a different amount of water was removed from the test tray. Upon completion the five samples were weighed and the result plotted against the difference between each corresponding set of balance readings.

After calibration of the weighing system, the test area access door and the water line clamp were closed. The access door in the tunnel inlet section was opened and the desired relative humidity sensor plugged into the receptacle whereupon the door was closed.

The desired air temperature in the tunnel was obtained by setting the thermostat on the refrigeration unit. The fan was started and the air velocity control gate adjusted to produce the

desired air speed. During the initial transient conditions the clamp on the plastic tubing was opened and water was added to the reservoir tray to compensate for the slight static pressure increase acting on the surface of the mass-transfer tray. This was accomplished by observing through the plastic window in the access door, the level of the water surface in the mass-transfer tray. The adjustment was completed when a thin film of water was visible over the entire cloth surface.

When the water surface temperature at location 1 (Figure 12) reached approximately 55 degrees F, the DC power supply units were turned on. The quantity of current flowing to the heating wire was adjusted so that the water surface temperature was maintained at about 51 degrees F. The system was allowed to run for a few minutes without further adjustment to insure that steady-state conditions had been attained.

The 30 minute duration test run was then started by positioning the event market on a particular time division on the chart, and closing the water line clamp. A balance reading was then made, the tray returned to its starting position and the clamp opened. At 5 minute intervals during the test run velocity, relative humidity, and water surface temperature (at all six locations) readings were taken. A continuous recording of air temperature was made with pen number one of the strip chart recorder. At precisely 30 minutes

after the start of the test run the water line clamp was closed and a balance reading (with the fan in operation) obtained. The difference between the initial and final balance reading was calculated and the actual quantity of water removed from the mass-transfer tray obtained from the weight calibration curve (Figure 29).

This procedure was repeated for different velocities and air temperatures.

5.3 Sprinkling the Leaf Model

The independent variables and their range of values studied in Phase Three of the investigation were:

a. air velocity (65 to 703 ft/min)

b. air temperature (13.9 to 27.7 F)

c. relative humidity of the air (36 to 66 percent)

d. change in sprinkled water temperature (2.5 to 10.0 F)

e. local plate surface temperatures (32.5 to 54.3 F)

The water application rate for a flat plate was measured for various values of the above variables. A total of 4 test series comprising 23 tests were run.

The leaf model mounted on its test stand was positioned in the center of the collector pan and adjusted until its surface was level and vertically in the center of the tunnel test area. Once this arrangement was completed, the location of the test stand was marked

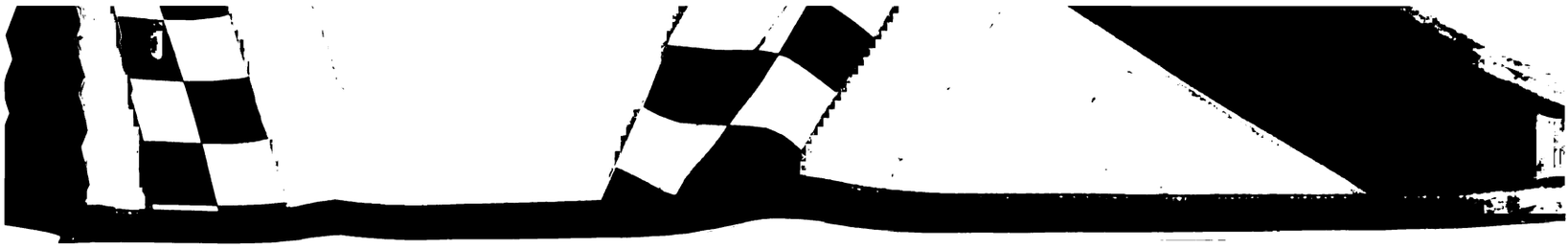

in the collector pan assuring proper alignment of the leaf model upon removal and replacement. The plastic tray used to determine the sprinkling rate was adjusted and its location marked so that its surface intercepted the precipitation at the exact same location in the test area as did the leaf model.

The desired nozzle tip size was selected and by means of the access door on the sprinkling tower installed in the nozzle assembly.

The desired air temperature in the tunnel was obtained by setting the thermostat on the cold storage box refrigeration unit. The fan was started and the desired air velocity obtained by adjusting the air intake gate.

The water line shut-off valve was turned on and the water pressure at the spray nozzle set at 10 lb/in.^{2} by adjusting the pressure regulator. A flood light mounted outside the window of the test area access door was turned on to allow visual observation of the leaf model during sprinkling. The primary reason for the visual observation was to assure that an approximately equal quantity of water was being discharged from each of the three collector trough outlets.

Once the air temperature in the test area had reached steady state, recordings of the six water temperatures in the collector trough, the three temperatures of the water film on the plate surface, and the three temperatures of the bottom plate surface were made by switching the two six-point manual switches to each position for a

brief time interval. During this same time the temperature of the air approaching the test area along with the water temperature at the spray nozzle and in the collector pan was recorded by the 16 point recorder. The air temperature downwind from the test area was not recorded due to the "icing-up" of the junction and subsequent invalid readings. Immediately following the temperature measurements an air velocity measurement was made with the hot-wire anemometer along with a relative humidity measurement. A visual check was then made of the leaf model and the spray nozzle water pressure and the above procedure repeated for a second time, thus affording two replications per test. With the spray shut off the leaf model was removed from the test area and the sprinkling rate calibration tray installed in its place. The lead wires from the two thermocouples in the tray were connected to the two pen strip chart recorder. The spray was then turned on for a period of 5 minutes, the time period was observed by stop watch. During this 5 minute period the air velocity and temperature were identical to those occurring during the sprinkling of the leaf model. The quantity of water collected in the tray was weighed to 0.1 of a gram on a Mettler Balance and the calibration procedure repeated a second time.

This procedure was then repeated for different air velocities, air temperatures, and sprinkling rates.

VI. DISCUSSION OF RESULTS

Prior to conducting the actual tests for each phase of the study the percent of free stream turbulence in the test area was determined. The measured free stream turbulence ranged from 2.9 percent at low velocities (100 ft/min) to 4.0 percent at high velocities (1000 ft/min).

6.1 Convection

The experimental data obtained for this phase of the study showed that the temperature of the plate surface increased with distance from the leading edge (Figure 28). It was observed that during any given test thermocouples 4 and 5 (Figure 8) indicated within 0.5 F of the same temperature as thermocouple 3. This confirmed the two-dimensionality of the thermal boundary layer development (constant in the z direction).

On the basis of equation (3.2.17) the values for the average Nusselt number for each test can be obtained from the relation

$$\overline{Nu} = \frac{Q_e \, L}{2A \, k \, \Delta T_p}, \qquad (6.1.1)$$

where Q_e is the total measured quantity of heat being removed from the plate per unit time (Btu/min) during any given test. The equation defining Q_e is

$$Q_e = (0.5692)\ V\ I \qquad (6.1.2)$$

where V is the voltage to the heating wire and I the amperage.

The results for this phase of the investigation are presented in Table 1 and in Figure 18. In Figure 18 the experimentally obtained values for convective heat transfer from a flat plate are compared to the values obtained using the theoretical equations for a constant plate surface temperature and a continuously varying plate surface temperature. This comparison is made by plotting the Nusselt number against the Reynolds number on log-log paper. From a least squares analysis the regression equation for the experimental data is

$$\overline{Nu} = .719\ Re_L^{0.494} \qquad (6.1.3)$$

The standard error of estimate SE_y, which is a measure of the amount of variation from the regression line based on ordinate values is ± 1.022. The equation for the average coefficient of convection obtained from curve (2), Figure 18, is

$$\overline{h}_c = .757\ \frac{k}{L}\ Re_L^{1/2}\ Pr^{1/3} \qquad (6.1.4)$$

Table 1.--Summary of convection tests.

Test No.	T_a F	U_a ft/min	Q_e Btu/min	$\Delta T_p'$ F	T_m F	$Re_L \times 10^{-3}$	$Re_L^{1/2}$	(1) $\overline{Nu}$	(2) $\overline{Nu}$	(3) $\overline{Nu}$
1	25.0	50.6	.081	8.33	28.3	2.94	54.2	40.54	38.3	32.30
2	21.0	79.3	.148	13.30	26.2	4.65	68.3	51.09	44.3	40.71
3	20.7	69.9	.146	13.80	26.1	4.10	64.2	48.02	42.1	38.26
4	18.5	101	.242	18.25	25.6	5.93	77.1	57.67	52.7	45.92
5	16.7	107	.270	19.42	24.2	6.31	79.6	59.54	55.2	47.44
6	15.0	139	.354	22.65	23.7	8.21	90.8	67.92	62.2	54.12
7	14.0	200	.438	23.34	23.1	11.83	108.9	81.46	74.7	64.90
8	13.0	228	.522	26.33	22.9	13.51	116.2	86.92	79.0	69.26
9	12.6	269	.537	24.77	22.4	15.96	126.2	94.40	86.5	75.22
10	12.1	309	.613	26.80	22.5	18.33	135.3	101.20	91.3	80.64
11	11.9	353	.664	26.84	22.5	20.94	144.5	108.09	98.6	86.12
12	11.3	406	.735	27.82	22.2	24.11	155.2	116.09	105.4	92.50
13	11.1	472	.735	26.20	21.8	28.06	167.8	125.51	112.0	100.00
14	11.0	504	.847	28.59	22.2	29.93	173.0	129.40	118.3	103.11
15	10.9	587	.935	30.07	22.5	34.82	186.9	139.80	123.9	111.39
16	10.8	603	.955	29.63	22.4	35.77	189.2	141.52	128.6	112.76
17	10.5	678	.997	29.69	22.4	40.21	201	150.35	133.9	119.80
18	10.3	777	1.077	30.24	22.5	46.09	215	160.82	142.1	128.14
19	10.1	961	1.243	31.19	22.3	57.00	239	178.77	160.0	142.44

(1) Theoretical values for a continuously varying plate surface temperature defined by eq. (3.2.14).

(2) Experimental values, defined by equation (6.1.1).

(3) Theoretical values for a constant plate surface temperature defined by eq. (3.2.3).

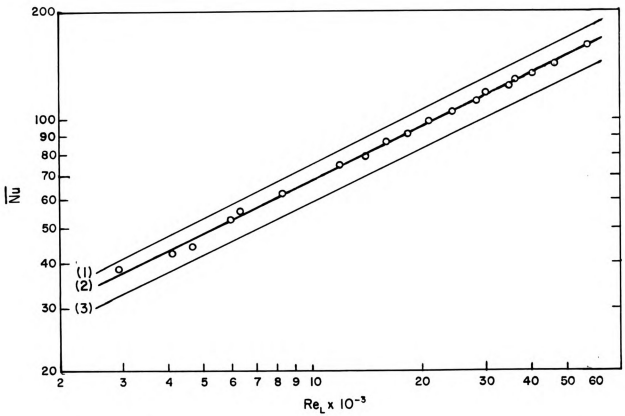

Figure 18.--Comparison of measured and calculated average film heat-transfer coefficients in laminar flow over a flat plate. Curve (1) for a continuously varying surface temperature was obtained with equation (3.2.14). Curve (2) is obtained from the measured values. Curve (3) for a constant plate surface temperature was obtained with equation (3.2.3).

Regression equation (2): $\overline{Nu} = .719\ Re_L^{0.494}$

Standard error of estimate = ± 1.022

It should be pointed out that at the maximum air velocity encountered of 961 fpm and free stream turbulence of 4.0 percent, the Reynolds number based on the total plate length was 57×10^3. Investigations by Edwards and Furber (1956) show that with 3.8 percent free stream turbulence the critical Reynolds number did not occur until a value of 80×10^3 was attained. Thus, during all the tests the air flow regime over the plate surfaces was laminar. This condition can also be verified for the tests conducted in Phase Two and Three.

Figure 18 shows excellent correlation among the experimental values. The actual measured rates of heat transfer as represented by the Nusselt number was 12.4 percent greater than those predicted by constant surface temperature theory but 5.8 percent less than those predicted by continuously varying surface temperature theory.

6.2 Mass-Transfer

Modification of equation (3.3.2) was necessary before it could be used in analyzing the test data. This equation is applicable only for a flat surface with a free water surface starting at the leading edge. The free water surface of the mass-transfer device used in this study starts a distance of 0.188 ft back of the leading edge. To account for this, the following equation for the average

coefficient of mass-transfer from Eckert and Drake (1959) is used.

$$\bar{h}_m = .664 \frac{D}{L} Re_L^{1/2} Sc^{1/3} \frac{1}{\left[1 - \left(x_o/L\right)^{3/4}\right]^{1/3}} \qquad (6.2.1)$$

L in this equation is measured from the leading edge to the inside back edge of the tray where the free water surface ends, a distance of 0.766 ft. Entering the stated values for x_o and L into equation (6.2.1) results in the relationship

$$\bar{h}_m = .679 \frac{D}{L} Re_L^{1/2} Sc^{1/3} \qquad (6.2.2)$$

The data from the balance calibration run preceding each test was combined into a single calibration curve shown in Figure 29. The regression equation for the line is

Actual Weight = 1.397 (Balance Reading Difference) - 0.221

with $SE_y = \pm .1772$

The results for this phase of the investigation are presented in Table 2 and Figure 19. In Figure 19 the experimental values, which are denoted by the circles, are compared to the theoretical curve which was calculated from equation (B.1.2.3) The measured values, although somewhat scattered, show good correlation with those predicted theoretically.

Table 2.--Summary of mass-transfer tests.

Test No.	U_a	RH	T_s	T_a	T	T_m	P_s	P_a	$Re_L X10^{-3}$	(1) M_s	(2) M_s	(3) Nm	(4) Nm
	ft/min	%	F	F	R	F	in./Hg	in./Hg		gm	gm		
1	866	62	43.4	19.1	503.4	31.3	.283	.061	76.60	7.13	6.25	152.91	134.32
2	465	63	43.6	15.5	503.6	29.6	.285	.052	41.27	5.44	4.75	112.06	98.06
3	465	63	43.6	15.1	503.6	29.4	.285	.051	41.27	5.46	5.00	112.06	102.75
4	830	62	47.5	22.1	504.8	33.6	.330	.071	73.16	8.09	8.76	149.60	160.38
5	221	40	50.1	17.3	510.1	33.7	.364	.036	19.50	5.27	5.01	76.88	73.21
6	161	63	50.3	20.8	510.3	35.6	.367	.067	14.03	4.13	4.19	65.47	66.50

(1) Theoretical values calculated from equation (B.1.2.2).

(2) Experimental values.

(3) Theoretical values calculated from equation (B.1.2.3).

(4) Experimental values calculated from equation (B.1.2.4)

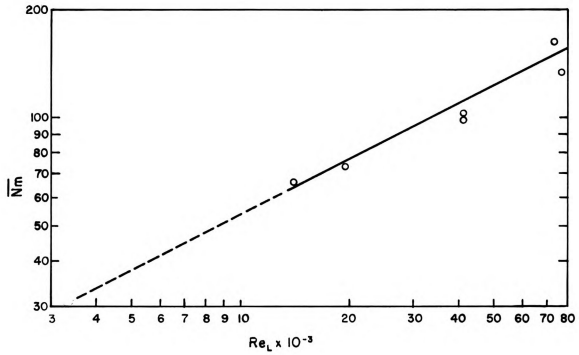

Figure 19.--Dimensionless mass-transfer coefficient for a flat surface evaporating water into a laminar air flow. The circles indicate the measured values. The curve is calculated from equation (B.1.2.3).

6.3 Sprinkling the Leaf Model

Three full-cone spray nozzles with orifice diameters of .024, .027, and .030 in. were operated at 10 psi to produce sprinkling rates ranging from .101 to .220 in./min with drop sizes varying between 0.2 and 1.0 mm in diameter.

The size of the water droplets at zero air velocity in the wind tunnel was determined by the process described by Engleman (1963). The procedure used was to briefly expose a 11 in. x 9 in. sheet of Ozalid 105SZ paper to the water spray followed by a brief exposure to ammonia fumes. The water spots, after drying, showed-up as yellow spots on a light gray (depending on the ammonia exposure time) background. The true diameter of the drops was calculated according to the empirical relationship

$$D = 0.43\ S^{0.74}$$

where D is the drop diameter in mm and S the spot diameter in mm.

The results for this phase of the investigation are presented in Table 3 and Figure 20. The theoretical water application rate was calculated from equation (3.4.3) where the average film heat-transfer coefficients for q_c', q_c, and q_m were obtained from Figure 18 [curve (2) and curve (3)] and Figure 19 respectively. In Figure 20 the measured water application rate is compared to the theoretical water application rate in the form of a dimensionless

Table 3.--Summary of sprinkling tests.

Test No.	ΔT_w F	T_s F	T_a F	T_m F	$\Delta T_p'$ F	T_m' F	RH %	U_a ft/min	$Re_L X10^{-3}$	$Re_L' X10^{-3}$	$\bar{h}_c'$	$\bar{h}_c$	$\bar{h}_m$	q_w	q_c'	q_m	q_c	w_e	w_t	$\frac{w_e}{w_t}$
											Btu/min ft^2 F		ft/min	Btu/min ft^2				in./min		
8	3.2	56.5	27.7	42.1	39.9	40.3	53	97	3.60	3.62	.029	.027	1.632	3.49	1.16	1.07	0.79	.210	.181	1.16
3	4.4	53.6	22.0	37.8	45.9	36.3	54	163	6.13	6.16	.038	.033	2.110	4.74	1.74	1.28	1.04	.207	.177	1.17
4	5.4	50.9	19.5	35.2	44.6	33.5	63	318	12.06	12.12	.053	.047	2.957	5.45	2.36	1.54	1.48	.194	.192	1.01
5	5.5	50.6	19.9	35.2	43.4	33.3	63	408	15.47	15.55	.060	.053	3.273	5.32	2.60	1.73	1.63	.186	.208	0.89
6	6.4	49.8	20.0	34.9	41.2	32.9	64	522	19.80	19.93	.067	.061	3.777	5.92	2.76	1.92	1.82	.178	.201	0.89
7	7.3	46.7	21.8	34.3	34.4	32.6	66	657	24.98	25.13	.076	.066	4.240	5.96	2.61	1.82	1.64	.157	.160	0.98
9	3.6	48.0	23.4	35.7	35.2	34.5	53	98	3.71	3.72	.029	.026	1.626	2.83	1.02	0.77	0.64	.151	.130	1.16
10	4.2	48.7	20.3	34.5	39.8	32.8	54	163	6.19	6.22	.038	.033	2.092	3.04	1.51	1.05	0.94	.139	.160	0.87
11	5.7	47.4	16.8	32.1	40.2	29.4	54	285	10.91	11.01	.050	.044	2.772	3.82	2.01	1.36	1.35	.129	.159	0.81
12	7.4	45.6	15.5	30.6	40.2	28.7	58	412	15.84	15.93	.060	.052	3.324	4.54	2.41	1.50	1.57	.118	.142	0.83
13	9.2	43.6	13.9	28.8	39.3	26.4	57	514	19.88	20.04	.067	.058	3.714	5.26	2.63	1.57	1.72	.110	.124	0.89
14	10.0	40.3	15.6	28.0	33.0	26.1	63	677	26.24	26.43	.078	.067	4.255	5.25	2.57	1.49	1.65	.101	.110	0.92
15	2.5	55.7	25.9	40.8	43.8	39.2	45	65	2.42	2.43	.024	.021	1.333	2.83	0.92	0.88	0.63	.218	.187	1.17
16	3.7	56.4	20.5	38.5	51.0	36.1	54	109	4.09	4.12	.031	.027	1.723	4.06	1.58	1.19	0.97	.211	.194	1.09
17	4.6	54.2	16.4	35.3	52.1	32.7	58	216	8.18	8.25	.044	.038	2.414	4.45	2.29	1.55	1.42	.186	.220	0.85
18	5.7	50.6	14.6	32.6	49.0	29.2	61	336	12.85	12.98	.054	.048	3.007	5.25	2.65	1.67	1.73	.177	.204	0.87
19	6.1	48.1	17.1	32.6	41.1	29.6	59	470	17.97	18.14	.064	.056	3.544	5.55	2.30	1.75	1.74	.175	.183	0.96
20	7.2	45.4	16.1	30.8	40.3	27.5	63	631	24.26	24.52	.074	.065	4.127	5.95	2.62	1.80	1.90	.159	.169	0.94
22	4.0	52.7	22.2	37.5	42.1	35.5	36	179	6.74	6.78	.040	.034	2.214	5.62	1.68	1.32	1.04	.220	.194	1.13
23	5.1	51.6	21.3	36.5	37.7	34.7	40	308	11.62	11.69	.052	.045	2.910	5.49	1.96	1.72	1.36	.207	.190	1.09
24	5.1	51.4	20.0	35.7	44.8	34.2	39	378	14.30	14.37	.058	.050	3.235	4.99	2.60	1.90	1.60	.188	.230	0.82
25	6.1	51.4	20.5	36.0	42.5	33.9	48	504	19.05	19.18	.066	.058	3.732	5.61	2.81	2.10	1.79	.177	.211	0.84
26	7.5	48.7	22.3	35.5	36.5	33.9	41	703	26.63	26.74	.079	.068	4.347	6.24	2.88	2.26	1.80	.160	.178	0.90

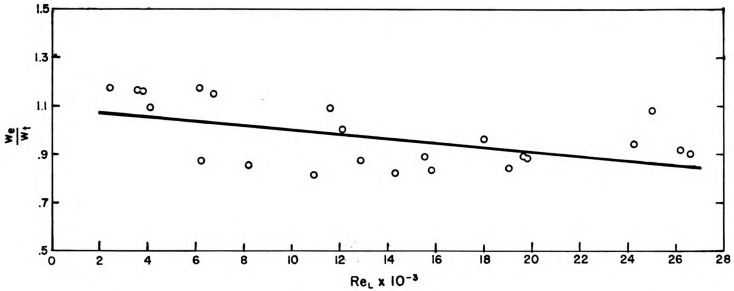

Figure 20.--A comparison of the experimental and theoretical water application rates.

Regression equation: $\frac{w_e}{w_t} = -9.24 \times 10^{-6} Re_L + 1.093$

Standard error of estimate = ± .1072

ratio plotted against Reynolds no. If there was perfect correlation, at least within the experimental accuracy of the test system, one would expect the ratio of w_e/w_t to be approximately one for all values of the Reynolds number. As indicated by Figure 20, this is not the case, values of w_e/w_t range from 0.81 to 1.17 for Reynolds numbers between 2×10^3 and 27×10^3. The regression equation for the least squares best-fit line is

$$\frac{w_e}{w_t} = -9.24 \times 10^{-6} \, Re_L + 1.093$$

with $SE_y = \pm .1072$

In examining the individual data points plotted in Figure 20 it was noted that primarily all w_e/w_t values of 1.1 or greater occur at low Reynolds numbers (up to 7×10^3). The values of w_e/w_t above 7×10^3 lie scattered about an approximate mean value of 0.90.

An attempt will now be made, first of all, to explain the occurrence of large w_e/w_t values at low Reynolds numbers. Visual observations of the plate surface during sprinkling indicated that maximum water film thickness occurs at minimum air velocity. As the air velocity increases the water film thickness decreases due to the drag of the air on the water surface. Also as the air velocity increased, the sprinkling rate decreased (see Table 3). The combined effects of high intensity precipitation striking a relatively thick

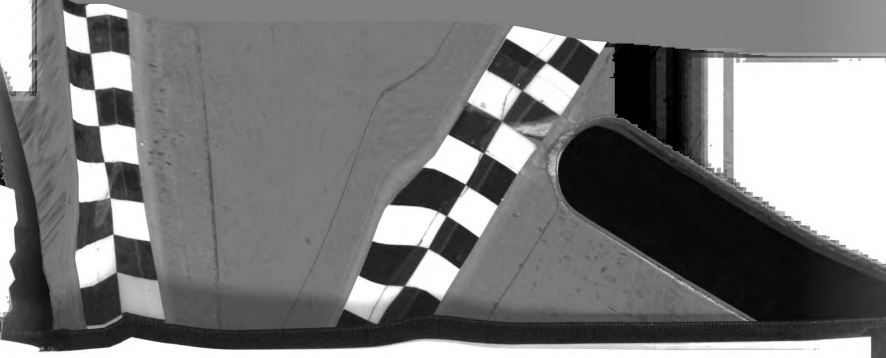

water film surface would tend to promote a very rough or "cratered" surface. Although exact theory pertaining to laminar air flow over rough surfaces is not available, intuitive thinking leaves little doubt that the coefficient of heat and mass transfer would be greater than that obtained for a smooth surface. This was brought about by the increased surface area and the "disturbed" (from the drops of falling water) nature of the boundary layer. Since the w_t values are derived for the case of laminar flow over smooth flat surfaces, these values would be lower than those actually occurring during the tests, hence the large values of w_e/w_t. The equation for w_t (3.4.3) also contains the heat loss term for the un-wetted underside of the plate. This term is not affected by the phenomina discussed here or in the following paragraph. As air velocity increased and water application rate decreased, this "surface cratering" effect would diminish.

In an attempt to explain why such a large portion of the remaining w_e/w_t values were below 0.90, an examination of the theory used in deriving the heat and mass transfer coefficients was made. These coefficients were derived for the boundary condition of zero air velocity at the plate surface. This condition no longer applies for the case of a moving water film on a flat plate since the air now has some finite velocity at the air-water interface. Appendix A contains an expression for the average coefficient of convective heat transfer derived for this boundary condition.

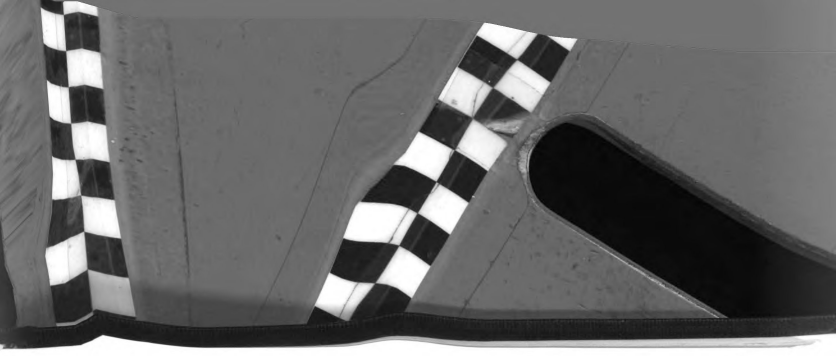

The resulting expression (A.1.11) is

$$\bar{h}_c = 0.398 \frac{k}{L} Pr^{1/3} (2Re_L + 3Re_l)^{1/2}$$

where Re_l, the Reynolds number, is defined in terms of the velocity at the air-water interface (u_l). The equation describing u_l (A.1.20) is

$$\frac{(u_a - u_l)(2u_a + 3u_l)^{1/2}}{u_l^2} = 37.03 \frac{\mu_w}{\mu_a} \left(\frac{\nu_a}{L}\right)^{1/2} \frac{1}{w}$$

where the a and w subscripts refer to air and water respectively. The derivation of this expression (see Appendix A) for u_l was based on certain assumptions concerning the water film on the plate surface. The validity of these assumptions was further borne out by observations and measurements made of the water film thickness b during sprinkling tests. The measured thickness of the thermocouple junctions lying on the plate surface averaged .040 in. During sprinkling tests at low air velocities, it was observed that the water film completely covered the thermocouple junctions, however at high velocities a portion of the junction protruded above the water film surface. A check of Table 4 shows that the water film thickness b ranged from a maximum of .088 in. with an air velocity of 65 fpm to a minimum of .011 in. with an air velocity of 677 fpm. The higher velocities did, however, tend to produce a non-uniform water film

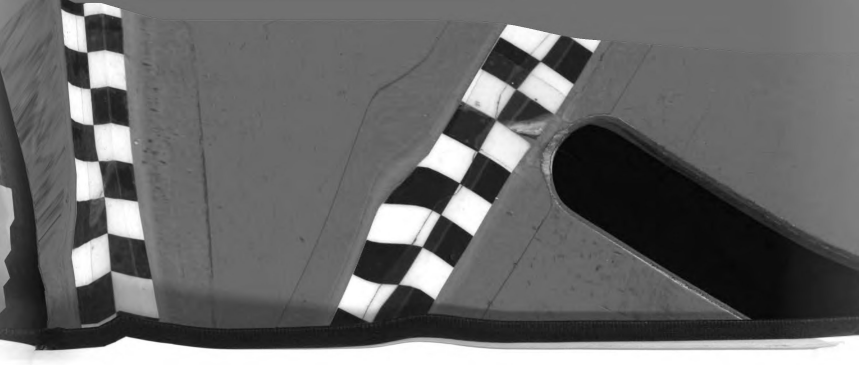

thickness by decreasing the depth near the leading edge of the plate and increasing it toward the back.

The average film heat-transfer coefficient over a moving water film [equation A.1.11)] includes the air-water interface velocity term u_1, which was not readily calculable. Since this expression for $\bar{h}_c$ differs by an almost constant amount (12.2 percent) from the $\bar{h}_c$ term for a flat plate without a water film (Figure 21) an expression was obtained for the moving water film heat-transfer coefficient which did not include u_1. This expression was

$$\bar{h}_c = .583 \frac{k}{L} Re_L^{1/2} Pr^{1/3} \qquad (6.3.1)$$

Similarly, the average coefficient of mass-transfer over a moving water film can be expressed as

$$\bar{h}_m = .583 \frac{D}{L} Re_L^{1/2} Sc^{1/3} \qquad (6.3.2)$$

The sprinkling data was re-evaluated using equations (6.3.1) and (6.3.2) for calculating the heat and mass transfer (assuming again the validity of the similarity relations proven in Phase Two) coefficients of the water film surface (heat loss expression for the bottom of the plate remaining unchanged). These results are shown in Table 4 and Figure 22 and 23. The measured values of the water application rate w_e were used in equation (A.1.20)

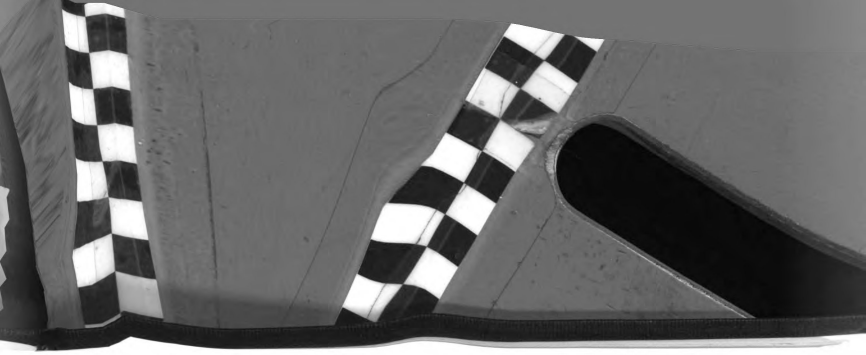

for evaluating u_1. In Figure 21 the values for the average Nusselt number are obtained by using equation (A.1.11) to define $\overline{h}_c$ [curve (4)]. The regression equation for the experimental points is

$$\overline{Nu} = .620\ Re_L^{0.481} \qquad \text{with } SE_y = \pm 1.010$$

Curve (3) in Figure 21 was obtained from equation (3.2.3) for the case of a flat plate without a water film on its surface. Comparison of curve (4) with curve (3) indicates that the values for the average Nusselt number are 11.2 percent ($Re_L = 2.25 \times 10^3$) to 13.2 percent ($Re_L = 30.00 \times 10^3$) less than those indicated by curve (3). The average value of 12.2 percent was used to reduce each of the q_c and q_m terms in Table 4 and subsequently obtain a second w_t value for each sprinkling test (Table 4). This value of w_t is compared with w_e in Figure 22 revealing that the values of w_e/w_t, with the exception of the few values occurring at low Reynolds numbers, are now scattered about an approximate mean value of 0.98 rather than 0.90 indicating better agreement between theory and experimentation. The regression equation for the experimental data is

$$w_e/w_t = -9.89 \times 10^{-6}\ Re_L + 1.173 \qquad \text{with } SE_y = \pm .1183$$

The dimensionless water application rate number defined by equation (3.4.4) was altered slightly. Since the mean temperature change experienced by the sprinkled water while on the leaf surface

Table 4.--Sprinkling data analyzed on the basis of the theoretical relationships developed for a flowing water film on a flat plate.

Test	u_a	u_l	b	$Re_L \times 10^{-3}$	$\overline{Nu}$ (1)	w_e	w_t	$\frac{w_e}{w_t}$	W
	ft/min		in.			in./min			
8	97	0.71	.066	3.60	31.80	.210	.168	1.25	9.02
3	163	1.04	.044	6.13	41.05	.207	.165	1.25	7.17
4	318	1.68	.026	12.06	57.03	.194	.178	1.09	5.73
5	408	2.08	.020	15.47	64.54	.186	.194	0.96	5.58
6	522	2.32	.017	19.80	70.58	.178	.187	0.95	4.80
7	657	2.59	.014	24.98	80.46	.157	.148	1.06	3.40
9	98	0.60	.056	3.71	31.83	.151	.121	1.25	6.85
10	163	0.85	.036	6.19	40.80	.139	.149	0.93	6.75
11	285	1.25	.023	10.91	53.72	.129	.148	0.87	5.36
12	412	1.57	.017	15.84	64.36	.118	.134	0.88	4.10
13	514	1.82	.013	19.88	71.91	.110	.115	0.96	3.22
14	677	2.12	.011	26.24	80.99	.101	.103	0.98	2.48
15	65	0.55	.088	2.42	26.27	.218	.173	1.26	11.92
16	109	0.78	.060	4.09	33.78	.211	.181	1.16	9.71
17	216	1.22	.034	8.18	47.06	.186	.205	0.91	8.22
18	336	1.67	.024	12.85	58.52	.177	.190	0.93	6.31
19	470	2.15	.018	17.97	69.06	.175	.169	1.04	5.08
20	631	2.55	.014	24.26	79.92	.159	.157	1.01	4.07
22	179	1.16	.042	6.74	43.08	.220	.180	1.22	7.61
23	308	1.68	.027	11.62	56.18	.207	.176	1.18	5.95
24	378	1.88	.022	14.30	62.02	.188	.214	0.88	6.16
25	504	2.19	.018	19.05	71.41	.177	.196	0.90	5.05
26	703	2.76	.013	26.63	84.12	.160	.165	0.97	4.19

(1) Calculated from equations (3.2.3) and (A.1.11) where $Re_a = Re_L$ and the fluid properties are evaluated at the mean value of T_m for all tests.

ΔT_w was difficult and impractical to measure it was replaced by the temperature difference $(T_s - T_a)$

$$W = \frac{5.20\, w_t\, Cp\, L\, (T_s - T_a)}{\overline{Nu'}\, k'\, \Delta T_p' + \overline{Nu}\, k\, (T_s - T_a) + \frac{\overline{Nm}\, H_v\, D\, (P_s - P_a)}{R\, T}} \qquad (6.3.3)$$

The dimensionless numbers $\overline{Nu'}$, $\overline{Nu}$, and $\overline{Nm}$ are obtained from Figures 18 [curve (2)], 21 [curve (4)], and 23 [curve (6)] respectively. In Figure 24 the dimensionless water application rate number is plotted against the Reynolds number of a log-log scale. The regression line is

$$W = 1159\, Re_L^{-0.526} \qquad \text{with } SE_y = \pm 1.192$$

To obtain the bottom plate surface temperature term $\Delta T_p'$ defined by equation (6.1.2) the local surface temperature at three locations (minimum) along the surface in the x direction must be measured and then a temperature profile curve (see Figure 30) plotted. To simplify the acquisition of this term, the following two empirical equations were derived from the test data (Figure 25):

For t_p at $x_1 = 0.169$ in. (x_1 measured from the leading edge)

$$\frac{\Delta T_p'}{(T_s - t_p)} = 61.28\, (Re_L / T_a)^{-0.353}, \quad \text{with } SE_y = \pm 1.159 \qquad (6.3.4)$$

For t_p at x_2 = 1.250 in. (x_2 measured from the leading edge)

$$\frac{\Delta T_p'}{(T_s - t_p)} = 98.83\,(Re_L/T_a)^{-0.379}, \quad \text{with } SE_y = \pm 1.210 \qquad (6.3.5)$$

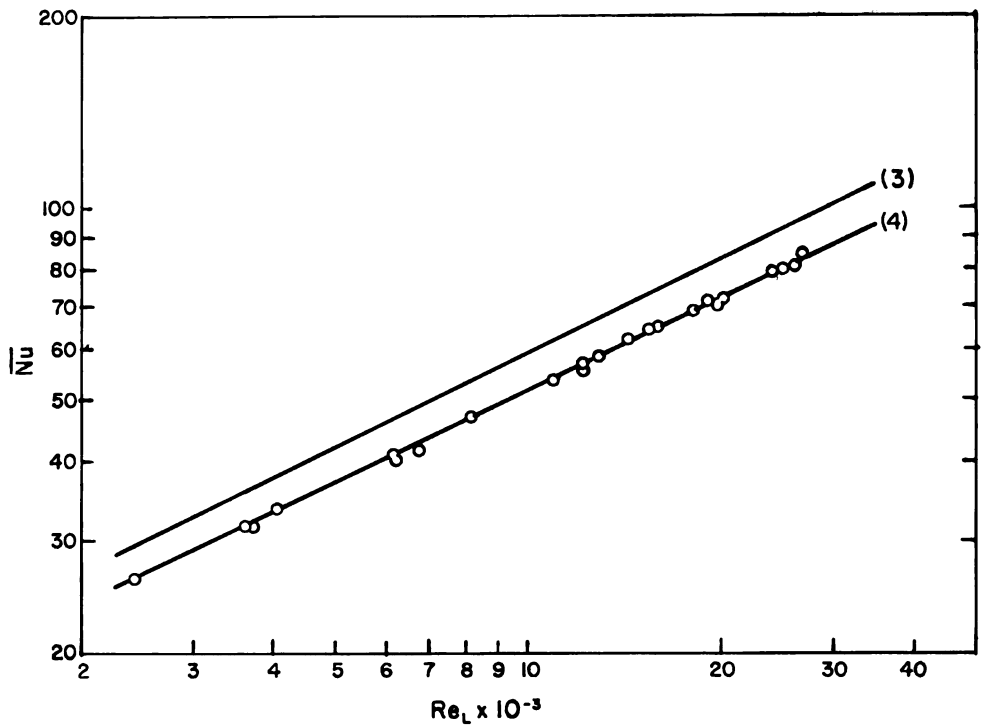

Figure 21.--Average film heat-transfer coefficients in laminar flow over a flat plate. Curve (3) was calculated with equation (3.2.3). Curve (4) was calculated using equation (A.1.11) for $\overline{h}_c$, which was derived for the case of a moving water film on the surface of a flat plate.

Regression equation (4): $\overline{Nu} = .620\ Re_L^{0.481}$

Standard error of estimate = ±1.010

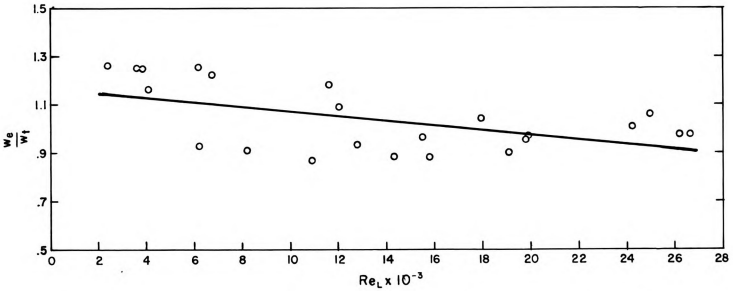

Figure 22.--A comparison of the experimental and theoretical water application rates. The theoretical water application rate was calculated for a flat plate covered by a moving water film.

Regression equation: $\frac{w_e}{w_t} = -9.89 \times 10^{-6} Re_L + 1.173$

Standard error of estimate = ± .1183

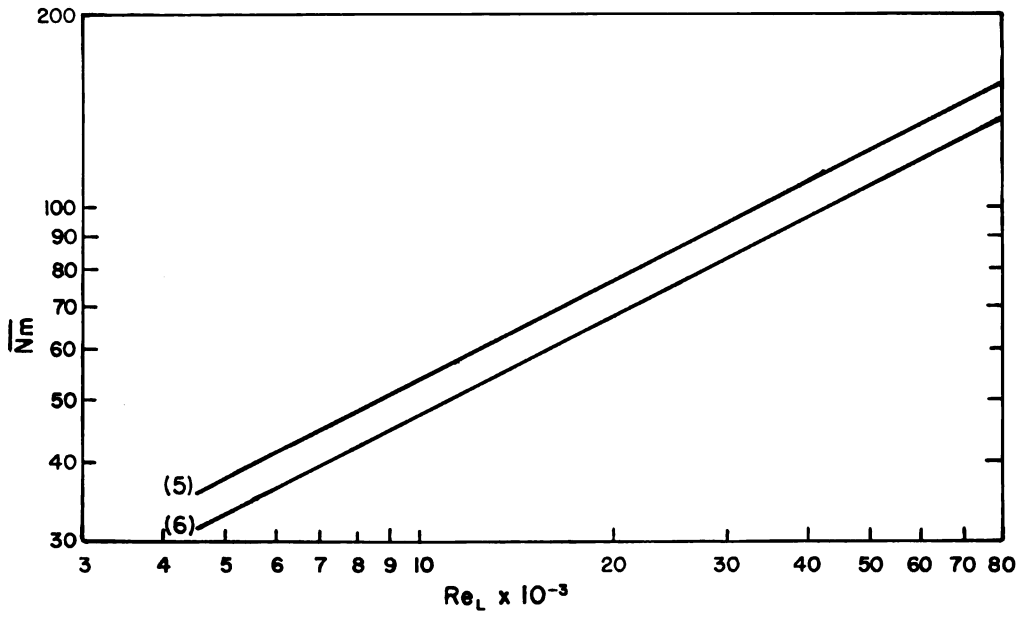

Figure 23.--Dimensionless mass-transfer coefficient for a flat surface evaporating water into a laminar air flow. Curve (5) calculated from equation (B.1.2.3) applies to a stationary water surface. Curve (6) calculated from equations (3.3.4) and (6.3.2) applies to a moving water film.

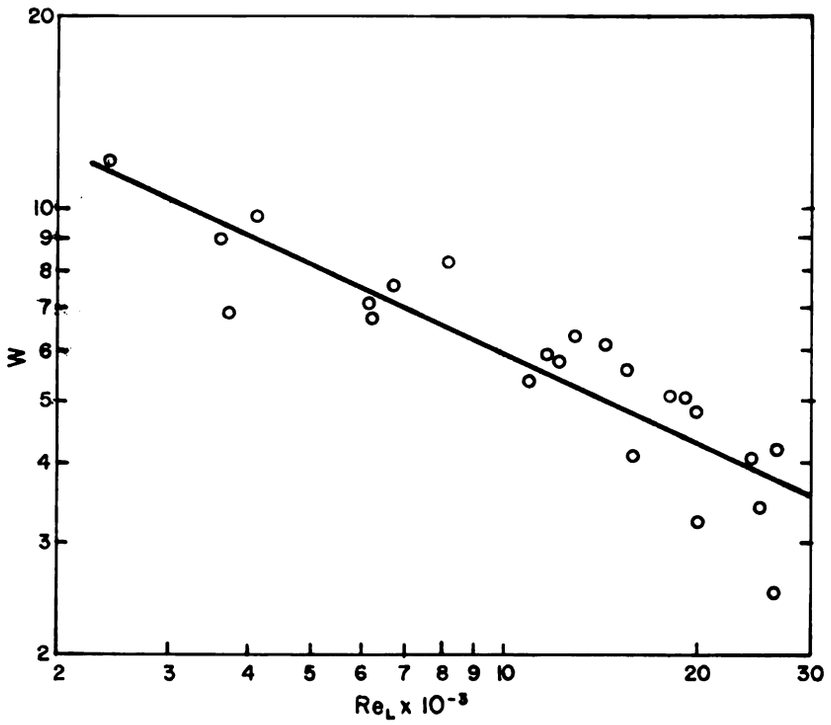

Figure 24.--Dimensionless water application rate number for the leaf model in laminar air flow parallel to its surface.

Regression equation: $W = 427.4\ Re_L^{-0.464}$

Standard error of estimate = ±1.192

$\Delta T_p'$

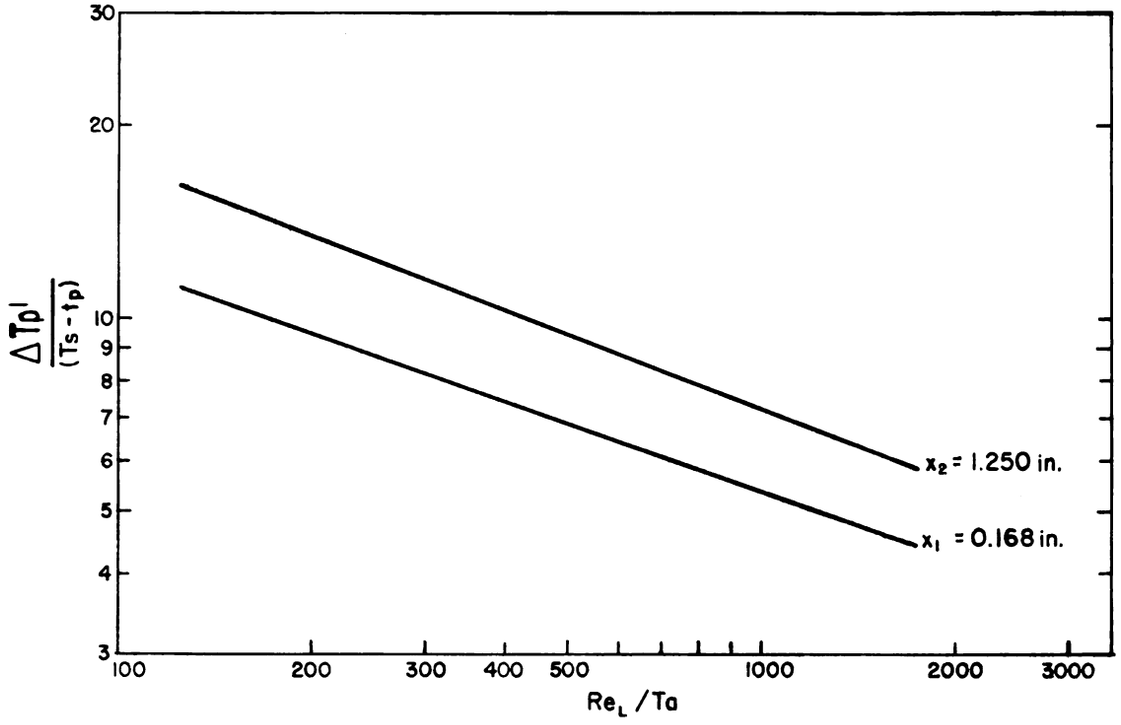

Figure 25.--Empirical correlation curve for determining $\Delta T_p'$ when the air, water film, and local plate temperatures are known.

Regression equation (x_1): $$\frac{\Delta T_p'}{T_s - t_p} = 61.28 \, (Re_L/T_a)^{-0.353}$$

Regression equation (x_2): $$\frac{\Delta T_p'}{T_s - t_p} = 98.83 \, (Re_L/T_a)^{-0.379}$$

Standard error of estimate (x_1) = ± 1.159
Standard error of estimate (x_2) = ± 1.210

VII. CONCLUSIONS

The correlation for the equations, determined experimentally in this study is expressed in terms of a plus or minus one standard deviation value. The limits represented by these values are obtained from the standard error of estimate and indicate that 68.27 percent of all values calculated by the prediction equations will fall within these limits.

The convective heat transfer coefficients $\bar{h}_c$ and $\bar{h}_c'$ defined by the equations which follow are expressed in units of Btu/min ft^2.

7.1 Convection

The rate of heat flow from a thin uniformly heated flat plate in laminar air flow can be calculated from the relationship

$$q_c' = \bar{h}_c \, \Delta T_p'$$

where

$$\bar{h}_c = .757 \frac{k}{L} \, Re_L^{1/2} \, Pr^{1/3} \pm .0007$$

and

$$\Delta T_p' = \Delta t_o + .969(\Delta t_n - \Delta t_o) - .432 \frac{\Delta L}{L}$$

$$\left[(2n-1)\ \Delta t_n - \Delta t_o - 2\sum_{n=o}^{n} \Delta t_n \right] \qquad (7.1.1)$$

7.2 Mass-Transfer

The rate of heat flow from a stationary free water surface due to water evaporating into a laminar air stream can be calculated from the relationship

$$q_m = \frac{\bar{h}_m H_v}{R T} (P_s - P_a)$$

where

$$\bar{h}_m = .664 \frac{D}{L} Re_L^{1/2} Sc^{1/3}$$

7.3 Sprinkling the Leaf Model

The quantity of heat removed from a continuously sprinkled leaf model in laminar air flow can be calculated from the relationships given in the following three paragraphs.

1. Convective heat loss from the un-wetted underside of the leaf model can not be accurately predicted by the constant surface temperature heat flow equation (3.2.4). The equation describing the heat loss was

$$q_c' = \left(.757 \frac{k}{L} Re_L^{1/2} Pr^{1/3} \pm .007\right) \Delta T_p'$$

$\Delta T_p'$ can be readily calculated from either of the empirical equations (6.3.4) or (6.3.5) depending on which local surface temperature is specified.

2. The coefficient of convective heat loss from the moving water film on the upper surface of the leaf model can best be predicted by equation (A.1.11) which accounts for the velocity at the air-water interface. Adjustment of equation (3.2.4) to account for this boundary condition results in a simplified relationship (elimination of the air-water interface velocity term u_1) for the convective heat loss.

$$q_c = \left(.583 \frac{k}{L} Re_L^{1/2} Pr^{1/3} \pm .0007\right) (T_s - T_a)$$

3. The equation describing the heat loss due to mass-transfer from a stationary water surface must be altered to account for the moving water film surface. This equation was

$$q_m = .583 \frac{H_v D}{R T L} Re_L^{1/2} Sc^{1/3} (P_s - P_a)$$

4. The sprinkling rate can be predicted from a dimensionless water application rate number formed by combining the above mentioned heat loss equations with the heat added equation (the sensible heat from the sprinkled water).

$$W = \frac{5.20\ w\ Cp\ L\ (T_s - T_a)}{q_c' + q_c + q_m}$$

W can be obtained from the plot of W versus Re_L (Figure 24) or from the regression equation

$$W = 1159\ Re_L^{-0.526} \pm 1.192$$

The results obtained from this study show that the constant-surface-temperature heat transfer equations postulated by Beahm (1959), Businger (1963), and others do not accurately predict the convective heat losses from the un-wetted under side of the leaf model. The constant-surface-temperature heat and mass transfer equations must also be altered slightly when used for predicting the heat loss from the flowing water film on the upper surface of the leaf model. The amount of alteration may be reduced to insignificance when the sprinkling rate is reduced to a value approximating that used in actual field practice. This, however, remains to be proven by future studies.

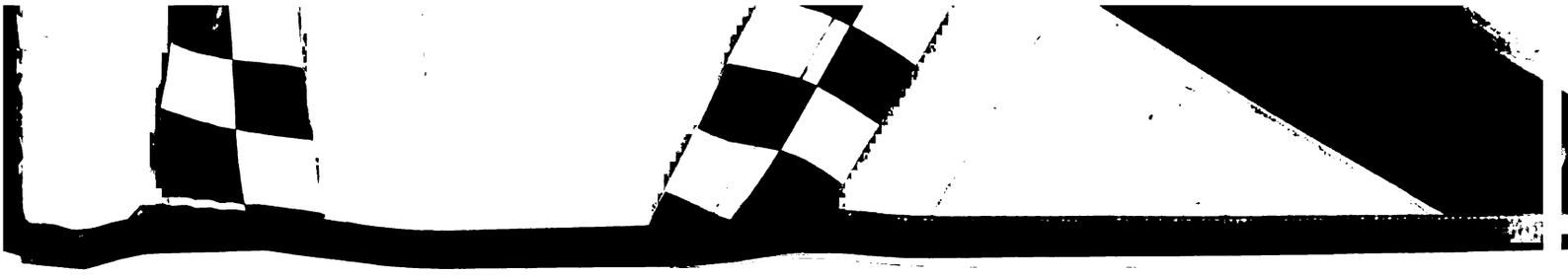

SUGGESTIONS FOR FUTURE STUDIES

This investigation has revealed the need for additional research in the following areas:

1. The applicability of the flat plate as a leaf model should be verified by sprinkling individual leaves under the same conditions imposed in this study. In addition, the radiation heat loss should be considered.

2. The effect which the angle of incidence has on the convection and mass-transfer terms in the prediction equation should be determined.

3. The effect of intermittent sprinkling, lower application rates, and drop size on the water application rate prediction equation should be analyzed.

4. The utilization of the latent heat of freezing of the sprinkled water accompanied by the surface ice load should be analyzed with respect to reducing the amount of water applied and any related changes which may occur in the heat transfer theory being applied.

APPENDIX A

A.1 Theoretical Derivation of the Average Film Heat-Transfer Coefficient Over a Flowing Water Film

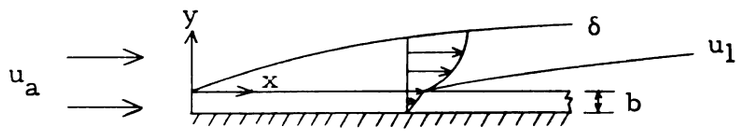

Figure 26.--Flow boundary layer over a water film on a flat plate.

Initially, the development of the hydrodynamic boundary layer over the surface of the water film will be considered. Assuming a second order polynomial to express the shape of the velocity profile:

$$u = A + By + Cy^2$$

From the boundary condition $u = u_l$ at $y = 0$ one obtains the equation

$$u_a = u_l + By + Cy^2$$

At $y = \delta$, $u = u_a$ thus

$$u_a = u_l + B\delta + C\delta^2 \qquad (A.1.1)$$

At $u = u_a$, $\frac{\partial u}{\partial y} = 0$ thus

$$0 = B + 2C\delta \tag{A.1.2}$$

Solving equations (A.1.1) and (A.1.2) simultaneously and rearranging terms results in the following expression for the velocity at any point in the hydrodynamic boundary layer.

$$\frac{u - u_1}{u_a - u_1} = \frac{2y}{\delta} - \frac{y^2}{\delta^2} \tag{A.1.3}$$

The integral momentum equation for the case of steady state, two-dimensional fluid flow with constant properties [Eckert and Drake (1959)] is

$$\frac{d}{dx} \int_o^\delta (u_a - u)\, u\, dy = \frac{\tau_o}{\rho} \tag{A.1.4}$$

In this equation the shear force at the water surface was evaluated as

$$\tau_o = \mu \left(\frac{du}{dy} \right)_{y=0} \tag{A.1.5}$$

Substituting for the value of u from equation (A.1.3)

$$\tau_o = \frac{2\mu\,(u_a - u_1)}{\delta\,\rho}$$

Substitution of equations (A.1.6) and (A.1.3) into the integral equation produces

$$\frac{d}{dx}\int_o^{\delta}\left[u_a - (u_a - u_1)\left(\frac{2y}{\delta} - \frac{y^2}{\delta^2}\right) - u_1\right]\left[(u_a - u_1)\left(\frac{2y}{\delta} - \frac{y^2}{\delta^2}\right) + u_1\right] dy$$

$$= \frac{2\mu\ (u_a - u_1)}{\delta\ \rho}$$

Letting $\eta = \frac{y}{\delta}$ one gets

$$(u_a - u_1)\ \frac{d}{dx}\ \delta\int_o^{\delta}\left[1 - 2\eta + \eta^2\right]\left[2\eta - \eta^2 + \frac{u_1}{u_a - u_1}\right] d\eta\ =\ \frac{2\nu}{\delta}$$

Expanding terms and integrating from 0 to 1

$$(u_a - u_1)\ \frac{d\delta}{dx}\ \frac{2}{15} + \frac{u_1}{3(u_a - u_1)}\ =\ \frac{2\nu}{\delta}$$

Separating variables and integrating

$$\delta^2\ =\ \frac{180\nu\ x}{6(u_a - u_1) + 5u_1} + C$$

At the leading edge of the water film x and δ are both zero, consequently $C = 0$.

The final expression for the boundary layer thickness is

$$\delta\ =\ x\left[\frac{60}{2Re_a + 3Re_1}\right]^{1/2} \qquad (A.1.7)$$

The local film heat-transfer coefficient for the water film surface is given by equation (3.2.11)

$$h_c = \frac{3}{2} \frac{k}{\zeta \delta} \qquad (A.1.8)$$

For a flat plate with a constant surface temperature Eckert and Drake (1959) give the following expression for ζ

$$\zeta = \frac{1}{1.026\ Pr^{1/3}} \qquad (A.2.9)$$

Substituting for ζ and δ in equation (A.1.8) and simplifying one obtains

$$h_c = 0.199 \frac{k}{x} Pr^{1/3} \ (2Re_a + 3Re_l)^{1/2} \qquad (A.1.10)$$

The average film heat-transfer coefficient is obtained by integrating equation (A.1.10) with respect to x from 0 to L.

$$\bar{h}_c = 0.398 \frac{k}{L} Pr^{1/3} \ (2Re_a + 3Re_l)^{1/2} \qquad (A.1.11)$$

This expression contains the unknown velocity of the water film surface u_l, which is a function of the free stream air velocity u_a and the water film thickness b. To arrive at an expression for u_l the condition of continuity of shear at the water film air interface is employed. The expression for the shear force on the air at the water surface is

$$\tau_a = \mu_a \left(\frac{du}{dy}\right)_{y=0}$$

where $\frac{du}{dy}$ is obtained from equation (A.1.3)

$$\tau_a = 2\mu_a \frac{(u_a - u_1)}{\delta}$$

Introducing equation (A.1.7) for δ and rearranging terms results in the following expression for shear,

$$\tau_a = \frac{0.258\ \mu_a\ (u_a - u_1)\ (2u_a + 3u_1)^{1/2}}{(\nu\ x)^{1/2}} \qquad (A.1.12)$$

The average shear over the water surface is obtained by integrating equation (A.1.12) with respect to x from 0 to L.

$$\bar{\tau}_a = 0.516 \left(\frac{L}{\nu}\right)^{1/2} \mu_a\ (u_a - u_1)\ (2u_a + 3u_1)^{1/2}$$

The shearing force within the water film is expressed as

$$\tau_w = \mu_w \left(\frac{du}{dy}\right)_{y = 0} \qquad (A.1.13)$$

where y is measured from the plate surface.

To obtain an expression for the velocity of the water u a linear velocity profile through the water film is assumed.

$$u = Dy + E$$

Assuming the boundary condition that at y = 0 u = 0 gives

$$u = Dy$$

At $y = b$ $u = u_1$ therefore

$$u = \frac{u_1 y}{b} \qquad (A.1.14)$$

By taking the derivative of this equation with respect to y, setting y equal to zero and substituting into equation (A.1.13) the relationship for τ_w is obtained.

$$\tau_w = \frac{\mu_w u_1}{b} \qquad (A.1.15)$$

The average shearing force over the surface is

$$\bar{\tau}_w = \int_o^L \tau_w \, dx = \mu_w u_1 \frac{L}{b} \qquad (A.1.16)$$

The two shearing forces, air and water, must be equal at the air-water interface.

$$\bar{\tau}_a = \bar{\tau}_w$$

$$.516 \left(\frac{L}{\nu}\right)^{1/2} \mu_a (u_a - u_1) (2u_a + 3u_1)^{1/2} = \frac{u_1 \mu_w L}{b} \qquad (A.1.17)$$

To arrive at an expression for the water layer thickness b in terms of known parameters it is assumed the water film flows only in the

x direction. Visual observation during actual sprinkling tests indicate that the flow pattern is such that approximately 1/3 of the water flows off the back of the plate at x = L with the remainder divided equally between the two sides.

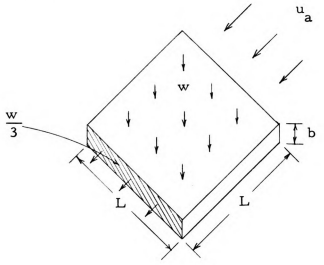

Figure 27.--Water film on a flat plate.

The quantity of water flowing out of the shaded element per unit time is

$$\frac{1}{3} Q_w = \int_o^b L\, u\, dy$$

Introducing equation (A.1.14) to express u

$$Q_w = 3 \int_o^b \frac{L\, u_1\, y}{b}\, dy$$

$$= \frac{3L\, u_1}{b} \int_o^b y\, dy$$

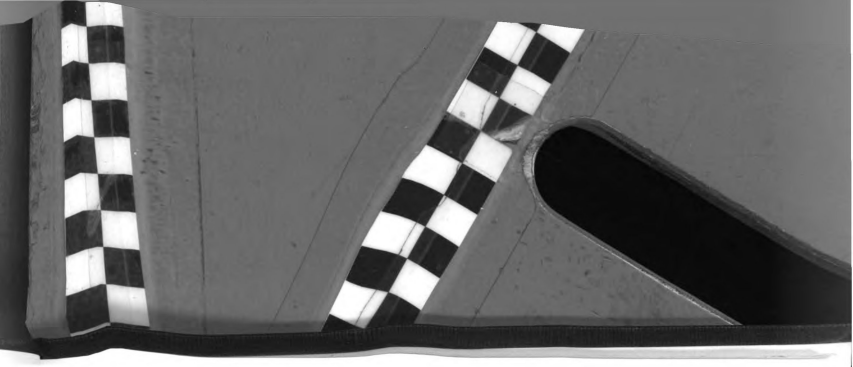

$$Q_w = \frac{3}{2} u_1 b L \quad (ft^3/min) \qquad (A.1.18)$$

The rate at which the water is leaving the plate must be equal to the rate at which water is applied to the plate by sprinkling.

$$\frac{3}{2} u_1 b L = \frac{w}{12} L^2$$

$$b = \frac{w L}{18 u_1} \qquad (A.1.19)$$

Introducing this expression for the water film thickness into equation (A.1.17) and simplifying provides an expression for u_1 in which all parameters are known.

$$\frac{(u_a - u_1)(2u_a + 3u_1)^{1/2}}{u_1^2} = 37.03 \frac{\mu_w}{\mu_a} \left(\frac{\nu_a}{L}\right)^2 \frac{1}{w} \qquad (A.1.20)$$

This equation can now be solved by the method of successive approximations or graphically for the velocity of the water, u_1, at the air-water interface. Inspection of equation (A.1.11) indicates that the value for the average coefficient of convection $\bar{h}_c$ will be smaller than that obtained by equation (3.2.2) (no water film on plate surface) even though the magnitude of u_1, as indicated by equation (A.1.20) is small compared to u_a.

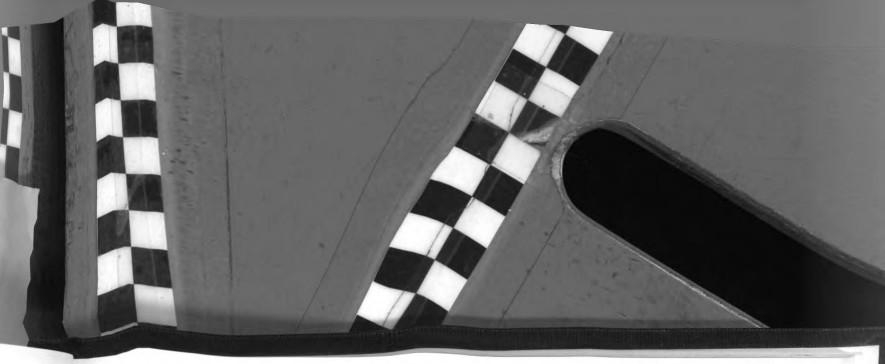

APPENDIX B

B.1 Sample Calculations

Sample calculations will be presented in accordance with the three separate and distinct phases of this investigation.

B.1.1 Convection

Test 8 will be used to demonstrate the calculations performed. For this test the following experimental data was obtained:

Plate Temperatures			Air Temperature	Heating Element		H.W. Current
t_1	t_2	t_3	T_a	V	I	4I
(F)	(F)	(F)	(F)	(volts)	(ma)	(ma)
31.1	33.7	34.2	13.0	34.3	268	616

From the hot-wire anemometer calibration curve

$$U_a = 288 \text{ ft/min}$$

The voltage and current to the plate heating element obtained from the calibration curves for the Weston analyzers are

$$V = 34.7 \text{ volts} \quad \text{and} \quad I = 272 \text{ ma}$$

The experimental value for the rate of heat transfer is calculated from equation (6.1.2)

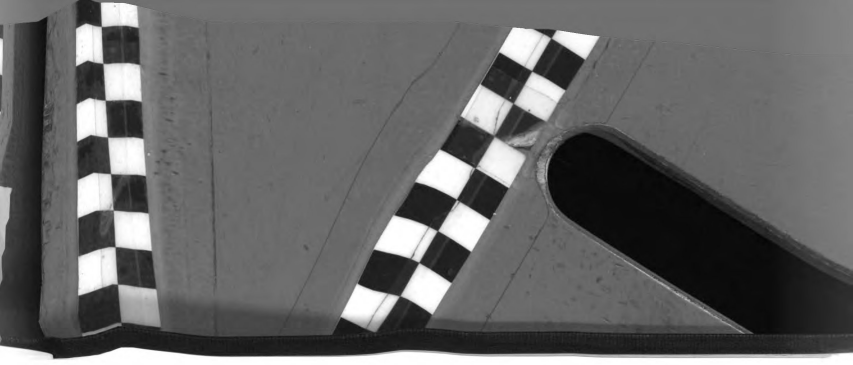

$$Q_e = (.05692)\ VI$$

$$= (.05692)\ (33.7)\ (.272)$$

$$= .522 \text{ Btu/min}$$

To evaluate $\Delta T_p'$, defined by equation (7.1.1), it is necessary to plot the plate surface temperature profile (Figure 28).

$$\Delta T_p' = \Delta t_o + .969(\Delta t_5 - \Delta t_o) - (.432)\frac{\Delta L}{L}\left[(2n-1)\Delta t_n - \Delta t_o - 2\sum_{n=o}^{n}\Delta t_n\right.$$

$$= 16.6 + .969(21.2 - 16.6) - (.432)\frac{.1}{.5}$$

$$\left[(10-1)\ 21.2 - 16.6 - 2\sum_{n=o}^{5} 124.9\right]$$

$$= 26.3 \text{ F}$$

The mean temperature used to evaluate the fluid properties was taken as

Tm = (average plate surface temperature + air temperature) $\frac{1}{2}$ = 22.9 F

Then

$$\nu = 8.44 \times 10^{-3} \text{ ft}^2/\text{min}$$

$$k = 22.98 \times 10^{-5} \text{ Btu/min ft}^2 \text{ F}$$

$$Pr = .72$$

The surface area of the plate includes the plate edge area and $\frac{2}{3}$ of the plate tab area.

$$A = .250 + .0208 + .002 = .271 \text{ ft}^2$$

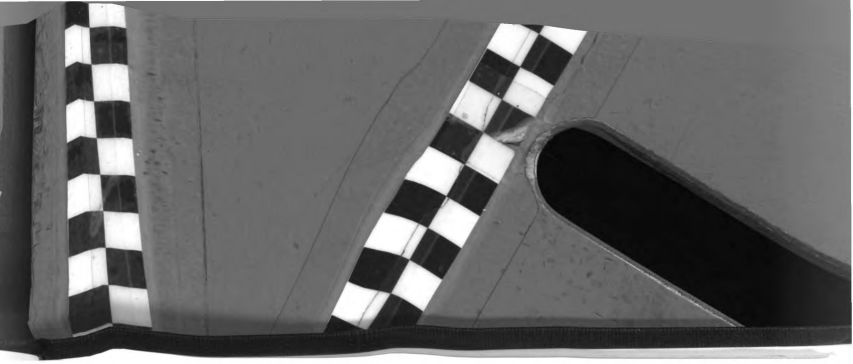

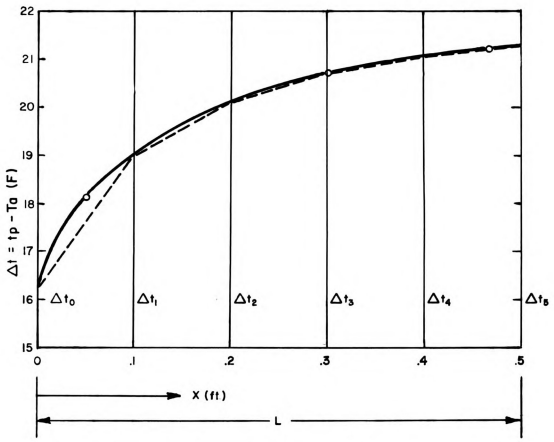

Figure 28.--Approximation of continuously varying plate surface temperature by straight line segments for convection test number 8.

Evaluating the Reynolds number

$$Re_L = \frac{U_a L}{\nu} = \frac{(228)\ (.5)}{8.44 \times 10^{-3}} = 13.51 \times 10^3$$

The theoretical Nusselt number for the case of a flat plate with a continuously varying surface temperature is given by equation (3.2.14) where $\bar{h}_c$ is defined by equation (3.2.13)

$$\overline{Nu} = .834\ Re_L^{1/2}\ Pr^{1/3}$$

$$= (.834)\ (13.507 \times 10^3)^{1/2}\ (.72)^{1/3}$$

$$= 86.92$$

The value of the theoretical Nusselt number for the case of a flat plate with a constant surface temperature is given by equation (3.2.3) where $\bar{h}_c$ is defined by equation (3.2.2).

$$\overline{Nu} = .664\ Re_L^{1/2}\ Pr^{1/3}$$

$$= (.664)\ (13.407 \times 10^3)^{1/2}\ (.72)^{1/3}$$

$$= 69.26$$

The experimental value of the Nusselt number is calculated from equation (6.1.1).

$$\overline{Nu} = \frac{(.522)\ (.5)}{(2)\ (.271)\ (22.98 \times 10^{-5})\ (26.3)} = 79.00$$

B.1.2 Mass-Transfer

Test 5 will be used to demonstrate the calculations performed. During the course of this test the following data was obtained:

Time (min)	4 I (ma)	RH (%)	T_a F	t_1 F	t_2 F	t_3 F	t_4 F	t_5 F	t_6 F
0	613	39	17.5	49.9	56.0	50.3	47.0	47.9	48.0
5			17.4	50.0	55.1	50.3	47.7	47.9	47.7
10			17.3	50.1	56.6	50.6	46.8	48.2	47.9
15	612	40	17.3	50.4	55.8	50.8	47.0	48.2	48.1
20			17.2	50.8	56.1	51.1	47.7	48.3	48.5
25			17.1	51.0	56.2	50.1	47.7	48.9	48.7
30	613	41	17.0	51.0	55.9	51.0	47.2	48.8	48.7

Balance reading difference = 3.75 gm

Averaging water surface temperatures with respect to time and location and air temperatures with respect to time one finds

$$T_s = 50.1 \text{ F}$$

$$T_a = 17.3 \text{ F}$$

The average absolute temperature of the water surface is

$$T = 510.1 \ ^{o}R$$

The mean temperature used to evaluate the fluid properties is

$$T_m = \frac{T_s + T_a}{2} = \frac{50.1 + 17.3}{2} = 33.7 \text{ F}$$

The vapor pressure at the water surface is the saturated vapor pressure of the air evaluated at the average water surface temperature.

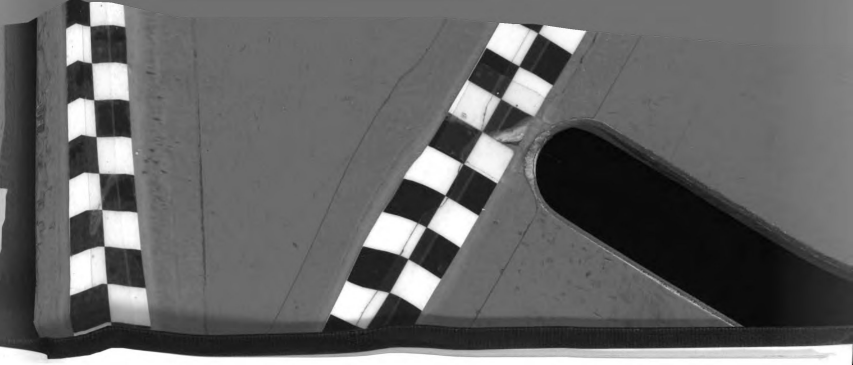

$$P_s = .364 \text{ in./Hg}$$

The vapor pressure of the free air stream is evaluated by determining the saturated vapor pressure of the air at the average air temperature and multiplying by the relative humidity.

$$P_a = (.40)\ (.089) = .036 \text{ in./Hg}$$

From the hot-wire anemometer calibration curve the average velocity is

$$U_a = 221 \text{ ft/min}$$

Evaluating the Reynolds number

$$Re_L = \frac{U_a\ L}{\nu} = \frac{(221)\ (.766)}{8.68 \times 10^{-3}} = 19.50 \times 10^3$$

Evaluating the Schmidt number

$$Sc = \frac{\nu}{D} = \frac{8.68 \times 10^{-3}}{16.31 \times 10^{-3}} = .532$$

The theoretical rate of mass-transfer is calculated from equations (3.3.1) and (6.2.1)

$$m_s = .664 \frac{D}{R\,T\,L}\ Re_L^{1/2} Sc^{1/3}\ (P_s - P_a)\ \frac{1}{\left[1-(xo/L)^{3/4}\right]^{1/3}} \quad (70.70)$$

(B.1.2.1)

The constant 70.70 converts the values of vapor pressure from in./Hg to lb/ft^2.

$$m_s = \frac{(.664)\,(16.31\times10^{-3})\,(19.5\times10^{3})^{1/2}(.532)^{1/3}(.364-.036)\,(70.70)}{(85.74)\,(510.1)\,(.766)} \cdot \frac{1}{\left[1-\left(.188/.766\right)^{3/4}\right]^{1/3}}$$

$$= .870 \times 10^{-3}\ lb/min\ ft^2$$

Converting the mass-transfer rate to the total quantity of water removed during the test one obtains

$$M_s = (m_s)\,(time)\,(area)\,(453.6) \qquad (B.1.2.2)$$

$$= (.870 \times 10^{-3})\,(30)\,(.444)\,(453.6)$$

$$= 5.27\ gm$$

The theoretical dimensionless mass-transfer number is given by equation (3.3.4) where $\overline{h}_m$ is defined by equation (6.2.2)

$$\overline{Nm} = (.679)\ Re_L^{1/2}\ Sc^{1/3} \qquad (B.1.2.3)$$

$$= (.679)\,(19.5 \times 10^{3})^{1/2}(.532)^{1/3}$$

$$= 76.88$$

The measured amount of water lost during the test is obtained from the balance calibration curve (Figure 29) as

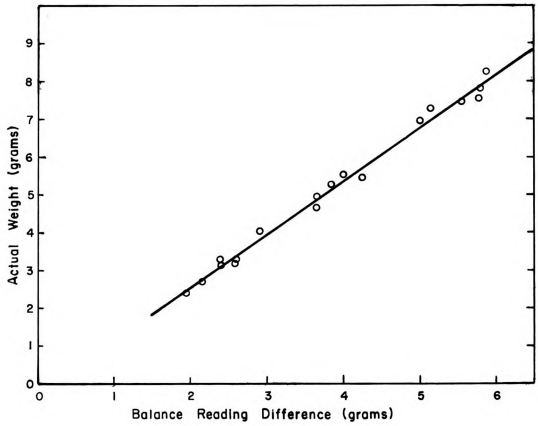

Figure 29.--Calibration curve for determining the quantity of water removed from the mass-transfer tray during a test.

Regression equation: Actual Weight = 1.397 (Bal. Reading Diff.) - 0.221

Standard error of estimate = ± .1772

$$m_s = 5.01 \text{ grams}$$

The experimental value for the dimensionless mass-transfer number is defined by the equation

$$\overline{Nm} = \frac{m_s \quad R \quad T \quad L}{(70.7)\,(D)\,(P_s - P_a)} \qquad (B.1.2.4)$$

Where m_s is the experimental mass-transfer rate evaluated as

$$m_s = \frac{M_s}{(.870 \times 10^{-3})\,(30)\,(.444)\,(453.6)}$$

$$= \frac{5.01}{6.04 \times 10^{3}}$$

$$= .829 \times 10^{-3} \text{ lb/min ft}^2$$

Substituting into equation (B.1.2.4) one obtains

$$\overline{Nm} = \frac{(.829 \times 10^{-3})\,(85.74)\,(510.1)\,(.766)}{(70.7)\,(16.31 \times 10^{-3})\,(.364 - .036)} = 73.21$$

B.1.3 Sprinkling the Leaf Model

Test 22 will be used to illustrate the calculations performed. For this test the following experimental data was obtained:

Average (from the six thermocouples in the collector troughs, with two replications) bulk temperature of the water leaving the plate

$$T_{w\text{-}off} = 49.3 \text{ F}$$

Average (from the three thermocouples on the plate surface, weighted according to surface area represented, with two replications) temperature of the water film

$$T_s = 52.7 \text{ F}$$

Average (two replicates) hot-wire anemometer reading is 677.5 ma.

Average (two replicates) relative humidity of the free airstream is 36 percent.

Average (two replicates) local plate surface (bottom) temperature:

x = .168 in.	x = 1.250 in.	x = 3.000 in.
46.1 F	47.8 F	52.2 F

Average (from two replicates) free stream air temperature is 22.2 F.

Average (from two five minute samples) weight of water collected in the application rate tray is 280.0 grams.

The change in temperature which the sprinkled water undergoes while on the plate surface was

$$\Delta T_w = T_{w\text{-on}} - T_{w\text{-off}} = 53.3 - 49.3 = 4.0 \text{ F}$$

The mean temperature used for evaluating the fluid properties of the water film surface was

$$T_m = \frac{T_s + T_a}{2} = \frac{52.7 + 22.2}{2} = 37.5 \text{ F}$$

Evaluation of $\Delta T_p'$, defined by equation (6.1.1) requires a plot of the bottom plate surface temperature profile (Figure 30).

$$\Delta T_p' = 23.6 + .969\ (29.4 - 23.6) - (.432)$$

$$\frac{.111}{.333}\ \left[(6 - 1)\ 29.4 - 23.6 - 2(106.2) \right]$$

$$= 42.1\ F$$

The mean temperature used for evaluating the fluid properties of the bottom plate surface was

$$T_m' = \frac{1/2\ (\Delta t_3 - \Delta t_o) + \Delta t_o + 2T_a}{2}$$

$$= \frac{1/2\ (29.4 - 23.6) + 23.6 + 2\ (22.2)}{2}$$

$$= 35.5\ F$$

The free stream air velocity obtained from the hot-wire anemometer calibration curve was

$$U_a = 179\ \text{ft/min}$$

Evaluating the Reynolds number for the water film surface

$$Re_L = \frac{U_a\ L}{\nu} = \frac{(179)\ (.333)}{8.85 \times 10^{-3}} = 6.74 \times 10^3$$

Evaluating the Reynolds number for the bottom plate surface

$$Re_L' = \frac{U_a\ L}{\nu'} = \frac{(179)\ (.333)}{8.79 \times 10^{-3}} = 6.78 \times 10^3$$

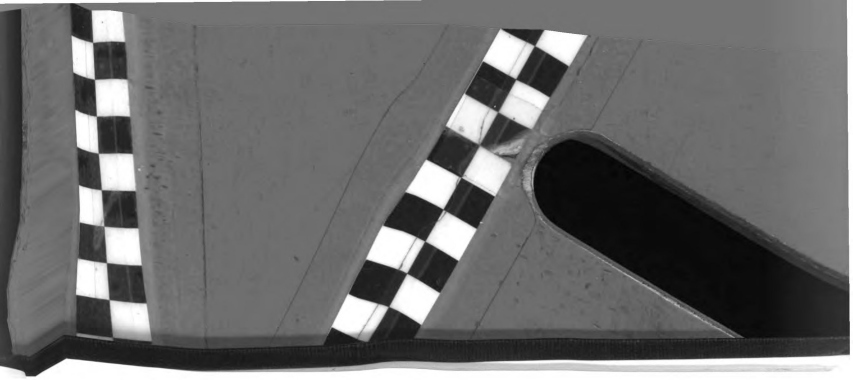

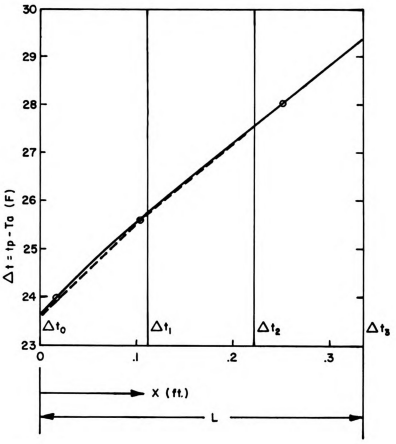

Figure 30.--Approximation of continuously varying plate surface temperature by straight line segments for sprinkling test 22.

The average coefficient of convection for the bottom plate surface is calculated from equation (3.2.14) where $\overline{Nu}$ is obtained from curve (2), Figure 18 knowing the value of Re_L'.

$$\bar{h}_c' = \frac{\overline{Nu}\, k'}{L}$$

$$= \frac{(56.5)\ (23.42 \times 10^{5})}{.333}$$

$$= .040 \text{ Btu/min ft}^2 \text{ F}$$

The rate of heat removal by convection from the bottom plate surface was calculated by equation (3.2.17)

$$q_c' = \bar{h}_c \Delta T_p' = (.040)\ (42.1) = 1.68 \text{ Btu/min ft}^2$$

The average coefficient of convection for the water film surface is calculated from equation (3.2.2) where $\overline{Nu}$ is obtained from curve (3), Figure 18 knowing the value of Re_L.

$$\bar{h}_c = \frac{\overline{Nu}\, k}{L}$$

$$= \frac{(48.5)\ (23.48 \times 10^{-5})}{.333}$$

$$= .034 \text{ Btu/min ft}^2 \text{ F}$$

The rate of heat removal by convection from the surface of the water film was calculated from equation (3.2.1)

$$q_c = \bar{h}_c\ (T_s - T_a) = .034\ (52.7 - 22.2) = 1.04 \text{ Btu/min ft}^2$$

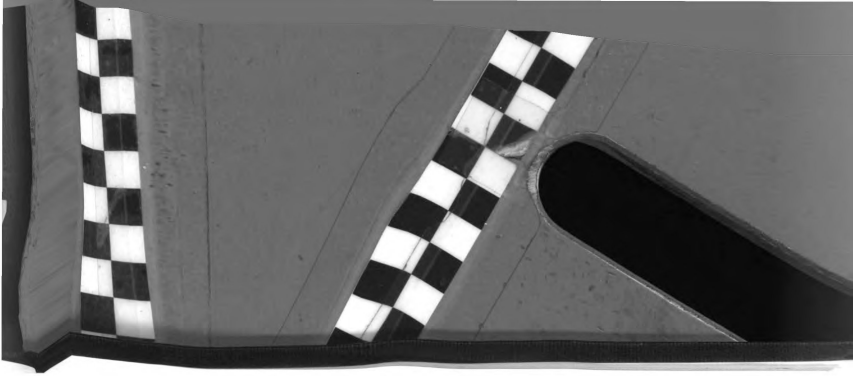

The average film heat-transfer coefficient for mass-transfer from the water film surface was calculated from equation (3.3.4) where $\overline{Nm}$ is obtained from Figure 19 knowing Re_L.

$$\bar{h}_m = \frac{\overline{Nm}\ D}{L} = \frac{(44.9)\ (16.57 \times 10^{-3})}{.333} = 2.214 \text{ ft/min}$$

The rate of heat removal accompanying the water film mass-transfer process was calculated from equation (3.3.5) and (3.3.1)

$$q_m = \frac{\bar{h}_m\ H_v}{R\ T}\ (P_s - P_a)$$

$$= \frac{(2.214)\ (1070)}{(85.7)\ (460 + 52.7)} \quad (24.46)$$

$$= 1.32 \text{ Btu/min ft}^2$$

The water application rate was determined from the relationship

$$w_e = \frac{(\text{weight of water})\ (12)}{(453.6)\ (62.4)\ (A)\ (\text{time})}$$

where the "weight of water" term is the adjusted average sample weight obtained from the application rate tray. It was found that when the actual weight of water for any series of tests (low to high velocity) was plotted against the air velocity (see Figure 31) a straight line relationship resulted. This relationship indicated that the weight of water collected and subsequently the application rate decreased as the air velocity increased. On the basis of this a

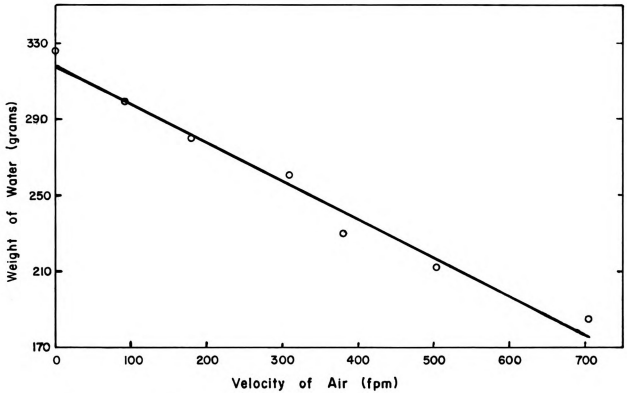

Figure 31.--The effect of air velocity on the quantity of water collected over a five minute period for sprinkling rate determinations (tests 21 through 26).

Regression equation: $Wt\ H_2O = -.202\ U_a + 318.3$

Standard error of estimation = ± 8.15

linear adjustment to the "weight of water" term was made to correct for the "Bernoulli" effect of the air velocity around the application rate tray. Since the tray had a face area (opposing the direction of air flow) that was 17.3 percent of the tunnel cross-section area, each original "weight of water" increment based on the quantity obtained at zero air velocity was increased by 17.3 percent.

$$w_e = \frac{(287.9)\quad(12)}{(453.6)\ (62.4)\ (.111)\ (5)} = .220 \text{ in/min.}$$

The rate at which heat was being added to the plate was calculated by equation (3.1.4).

$$q_w = 5.20\ w_e\ c_p\ \Delta T_w$$

$$= (5.20)\ (.220)\ (1.0)\ (4.0)$$

$$= 4.62 \text{ Btu/min ft}^2$$

The theoretical water application rate was calculated from the relationship

$$w_t = \frac{q_c' + q_c + q_m}{5.20\ \Delta T_w\ Cp} = \frac{1.68 + 1.04 + 1.32}{(5.20)(4.0)(1.0)} = .194 \text{ in./min}$$

The ratio of the experimental to theoretical application rate was then calculated as

$$\frac{w_e}{w_t} = \frac{.220}{.194} = 1.13$$

The dimensionless water application rate number (for a flowing water film on the plate surface) was calculated from the following relationship

$$W = \frac{5.20\ w_t\ Cp\ (T_s - T_a)}{q_c' + (q_c + q_m)\ (.878)} \qquad (B.1.3.1)$$

$$= \frac{(5.20)\ (.194)\ (1.0)\ (30.7)}{2.60 + (1.63+1.73)\ (.878)}$$

$$= 5.58$$

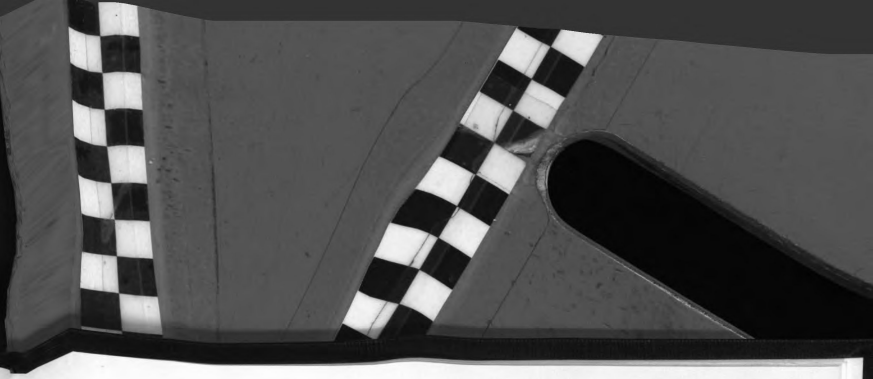

APPENDIX C

C.1 Propagation of Errors for the Theoretical Water Application Rate Equation

In this study and any related studies which may follow in the same area it is desirable to know what effect the precision of each independent variable measurement has on the accuracy of the dependent variable being predicted. This can be achieved by utilizing the propagation of error method of combining independent errors.

According to Mickley, Sherwood, and Reed (1957) the indirectly measured quantity (dependent variable) is a function of one or more directly measured quantities (independent variable).

$$Q = f(q_1, q_2, \ldots, q_n) \qquad (C.1.1)$$

The differential change in Q corresponding to a differential change in each of the q's is

$$dQ = \frac{\partial f}{\partial q_1} dq_1 + \frac{\partial f}{\partial q_2} dq_2 + \ldots \frac{\partial f}{\partial q_n} dq_n \qquad (C.1.2)$$

If the differentials $dq_1, dq_2, \ldots, dq_n$ are replaced by small finite increments $\delta q_2, \ldots, \delta q_n$ there results as a good approximation (assuming that the quantities δq are small so that all higher order terms in a Taylor's expansion of $Q + \delta Q$ are negligible) for

δQ the expression

$$\delta Q = \frac{\partial f}{\partial q_1} \delta q_1 + \frac{\partial f}{\partial q_2} \delta q_2 + \ldots + \frac{\partial f}{\partial q_n} \delta q_n \qquad (C.1.3)$$

The quantities δq_1, δq_2, . . . , δq_n may be considered as errors in q_1, q_2, . . . , q_n, and (C.1.3) provides a means of computing the resulting error in the function and the error contribution from each independent term.

The theoretical prediction equation for the dependent variable is

$$w = \frac{q_c' + q_c + q_m}{5.20\ Cp\ \Delta T_w} \qquad (C.1.4)$$

Introducing the expression for q_c', q_c, and q_m results in the expression

$$w = \frac{.757 Re_L^{1/2} Pr^{1/3} k' \Delta T_p' + .664 Re_L^{1/2} Pr^{1/3} k (T_s - T_a) + .664 Re_L^{1/2} Sc^{1/3} \frac{H_v D (P_s - P_a)}{RT}}{5.20\ Cp\ L\ \Delta T_w} \qquad (C.1.5)$$

Considering all dimension and fluid property terms as constant

$$w = \frac{A U_a^{1/2} \Delta T_p' + B U_a^{1/2} (T_s - T_a) + C U_a^{1/2} (P_s - P_a)}{\Delta T_w} \qquad (C.1.6)$$

where

$$A = \frac{.757\ Pr^{1/3}\ k'\ (L/\nu)^{1/2}}{5.20\ L\ Cp}$$

$$B = \frac{.664\ Pr^{1/3}\ k\ (L/\nu)^{1/2}}{5.20\ L\ Cp}$$

$$C = \frac{.664\ Sc^{1/3}\ H_v\ D\ (L/\nu)^{1/2}}{5.20\ L\ R\ Cp}$$

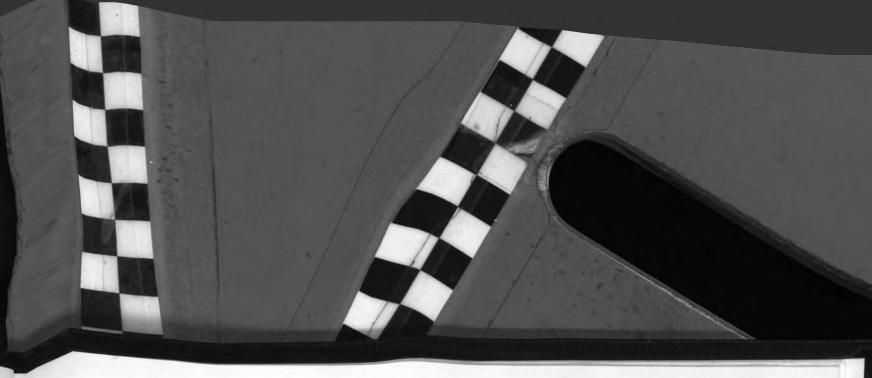

The saturated vapor pressure in lb/ft^2 can be expressed in terms of T_s as

$$P_s = 2.78 \exp\left[1.43 + \frac{17.25\, T_{sc}}{238 + T_{sc}}\right]$$

where T_{sc} is in degrees Centigrade.

The vapor pressure of the air in lb/ft^2 can be expressed in terms of T_a as

$$P_a = (RH)\, 2.78 \exp\left[1.43 + \frac{17.25\, T_{ac}}{238 + T_{ac}}\right]$$

where T_{ac} is in degrees Centigrade. With these two expressions for the vapor pressure, equation (C.1.6) becomes

$$w = \frac{A\, U_a^{1/2}\, \Delta T_p' + B\, U_a^{1/2}\, (T_s - T_a)}{\Delta T_w} + \frac{C\, U_a^{1/2}\, 2.78 \left[\exp\left(1.43 + \frac{17.25\, T_{sc}}{238 + T_{sc}}\right) - \exp\left(1.43 + \frac{17.25\, T_{ac}}{238 + T_{ac}}\right)\right]}{\Delta T_w} \qquad (C.1.9)$$

Taking $\Delta T_p'$ and ΔT_w as the difference between two temperature measurements the total derivative of equation (C.1.9) is

$$\delta w = A\left[\frac{\Delta T_p'}{2U_a^{1/2}\Delta T_w}\ \delta U_a\right] + B\left[\frac{T_s - T_a}{2U_a^{1/2}\Delta T_w}\ \delta U_a\right] + C\left\{\frac{P_s - P_a}{2U_a^{1/2}(460+T_s)\ \Delta T_w}\ \delta U_a\right.$$

$$+ \frac{U_a^{1/2}(P_s - P_a)}{(460+T_s)^2\ \Delta T_w}\ \delta T_s + \frac{U_a^{1/2}}{(460+T_s)\ \Delta T_w}\left[\frac{P_s}{(238+T_{sc})^2}\ (4110)\ \delta T_{sc}\right.$$

$$\left.\left. - P_a\ \delta(RH) - \frac{P_a}{(238+T_{ac})^2}\ (4110)\ \delta T_{ac}\right]\right\} \qquad (C.1.10)$$

The magnitude of the individual sources of error based on the values obtained for the independent variables in sprinkling test 26 are:

$\delta U_a = \pm 14.1$ ft / min

$\delta T_s = \pm .63$ F

$\delta T_{sc} = \pm .44$ C

$\delta T_a = \pm .63$ F

$\delta T_{ac} = \pm .44$ C

$\delta(RH) = \pm 3$ percent

The maximum error was obtained by determining the absolute value for each term (test 26) in equation (C.1.10) and combining those terms originating from the same source of error (indicated in parentheses by each value).

$$|\delta w| = \left[17.61\,(U_a) + 20.32\,(T_s) + 2.45\,(RH) + 3.18\,(T_a)\right] \times 10^{-4} \qquad (C.1.11)$$

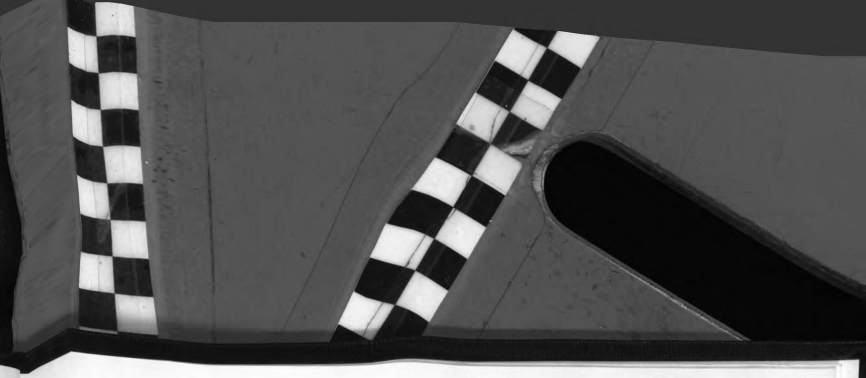

Thus the maximum (provided all errors occurred simultaneously at their maximum absolute values) possible error due to the precision of the instruments used to measure each independent variable is

$$|\delta w| = .0044 \text{ in./min}$$

or, expressed in another manner

$$w = .178 \pm 2.47 \text{ percent, in./hr}$$

Taking the δT_s error as one in equation (C.1.11) the relative order of magnitude of each error term is

$$\delta T_s \text{ - - - } 1.00$$

$$\delta U_a \text{ - - - } 0.87$$

$$\delta T_a \text{ - - - } 0.16$$

$$\delta(RH) \text{ - - } 0.12$$

The mean water film temperature and the air velocity must, therefore, be measured with a precision which is approximately, 7 times greater than that used to measure air temperature and relative humidity if one expects the same error contribution from each independent variable in the theoretical prediction equation for w.

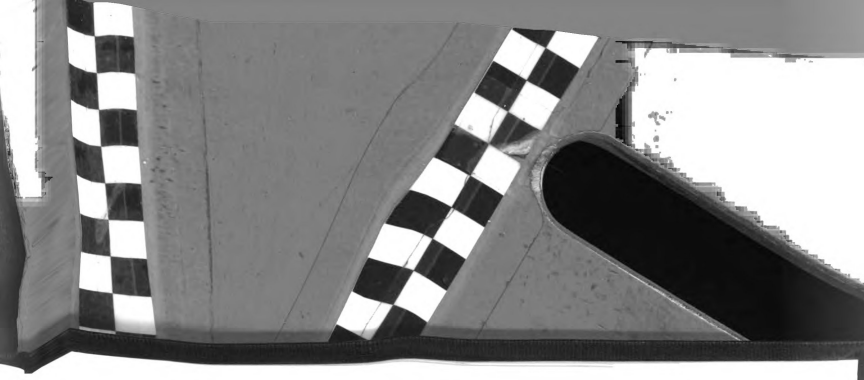

REFERENCES

Beahm, R. B.
1959 Experimental and theoretical study of frost protection by water application under simulated radiation frost conditions.
Thesis for the degree of M.S., Michigan State University, East Lansing (Unpublished).

Braud, H. Jr., and Hawthorne, P. L.
1965 Cold Protection for Louisiana Strawberries,
Agricultural Experiment Station Bulletin, No. 591.

Brouwer, W.
1959 Die Feldberegnung
DLG - Verlags-Gnbh, Frankfurt, West Germany.

Businger, J. A.
1963 Frost protection with irrigation.
Mimeograph of paper presented at 5th National Conference Agricultural Meeting, Lakeland, Florida.

Eckert, E. R. G. and Drake, R. M.
1959 Heat and Mass Transfer
McGraw-Hill Book Company, New York, N. Y.

Eckman, D. P.
1950 Industrial Instrumentation
John Wiley and Sons, New York, N. Y.

Edwards, A. and Furber, B. N
1956 The influence of free-stream turbulence on heat transfer by convection from an isolated region of a plane surface in parallel air flow.
Proc. Inst. Mechanical Engineer, 170; 141.

Engelman, R. J.
1963 Rain Scavenging of Particulates
AEC Research and Development Report,
HW-79382, pp. 28-26.

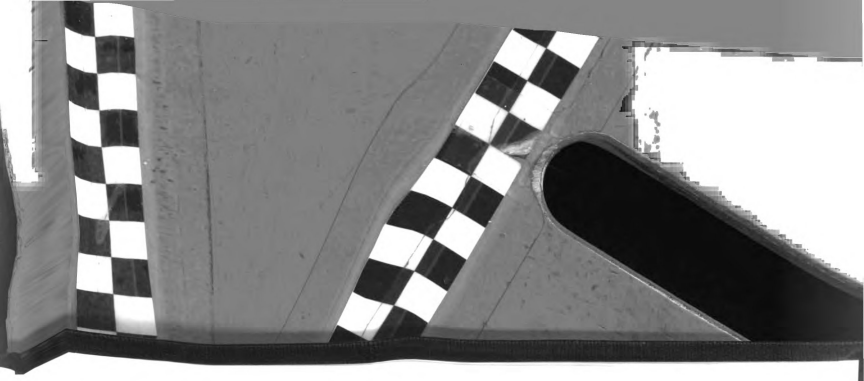

Flow Corporation
1958 Model HWB2 hot-wire anemometer theory and instruction. Flow Corporation Bulletin No. 37B.

Gates, D. M.
1962 Energy Exchange in the Biosphere. Harper and Row, New York.

Gates, D. M.
1962 Leaf temperature and energy exchange arch. Meterol. Geophys. U. Bioklimatol-Series B, 12:321-336.

Gates, D. M. and Bendict, C. M.
1963 Conduction phenomena from plants in still air. American Journal of Botany, 50: 563-573.

Gerber, J. F. and Harrison, D. S.
1963 Research with sprinkler irrigation for cold protection of citrus. Mimeograph of paper presented at the 1963 winter meeting of ASAE, Chicago, Illinois.

Hartnett, J. P. and Eckert, E. R. G.
1957 Mass-transfer cooling in a laminar boundary layer with constant fluid properties. Trans. ASME, 79:247-254.

Jakob, M.
1958 Heat Transfer. John Wiley and Sons, Inc., N. Y.

Kassler, O. W. and Kaempfort, W.
1949 Der Froslchadenverhutung. Reichskuratorium f. Techn. i.d. Landwirtsch. Wiss. Abh 6, No. 2.

Kidder, E. H. and Davis, J. R.
1956 Frost protection with sprinkler irrigation. Cooperative Extension Bulletin, Michigan State University, East Lansing, No. 327, (Revised).

Kreith, F.
1958 Principles of Heat Transfer. International Textbook Co., Scranton, Pa.

Mickley, H. S., Sherwood, T. K., and Reed, C. E.
1957 Applied Mathematics in Chemical Engineering.
Mc Graw-Hill Book Company, Inc., N. Y.

Niemann, A.
1958 Unterschunger zur physik der frostberegnung.
Wasser and Nahrung 2.

Perry, H. J. (editor)
1950 Chemical Engineers Handbook
Mc Graw-Hill Book Company, Inc., N. Y.

Raschke, K.
1960 Heat transfer between the plant and the environment.
Ann. Rev. of Plant Psysiol. 11:111-126.

Rogers, W. S.
1952 Some aspects of spring frost damage to fruit and its control.
Report of the thirteenth International Horticultural Congress.

Rogers, W. S., Modlibowska, I, Ruston, J. P., Slater, C. H. W.
1954 Low temperature injury to fruit blossoms. IV. Further experiments on water sprinkling as an antifrost measure.
Jour. Hort. Sci. 29:126-141.

Schlichting, H.
1960 Boundary Layer Theory.
Mc Graw-Hill Book Company, Inc., N. Y.

Schultz, H. G. and Parks, R. R.
1957 California Agricultural, Vol. 11, No. 6.

von Pogrell, H. and Kidder, E. H.
1959 Precipitation and drop size distribution from two medium pressure irrigation sprinklers.
Mich. Agr. Exp. Sta. Quart. Bul. 42:154-163

von Pogrell, H. and Kidder, E. H.
1959 The effectiveness of water use in sprinkling irrigation for frost protection.
Mich. Agr. Exp. Sta. Quart. Bul. 42:323-330.

Wheaton, R. Z.
1959 An experimental study of the effect of wind and water application factors on frost protection by sprinkling. Thesis for the Degree of M.S., Michigan State Univ. (Unpublished).